

**"BABEȘ-BOLYAI" UNIVERSITY OF CLUJ-NAPOCA
FACULTY OF CHEMISTRY AND CHEMICAL ENGINEERING
DEPARTMENT OF PHYSICAL CHEMISTRY**

VASILICA-DANIELA POP (TOADER)

**MODELING THE INTERACTIONS OF
SOME CHEMICAL COMPOUNDS WITH THE
LIPID MEMBRANES AND BIOMEMBRANES**

PhD Thesis Abstract

**Scientific advisor:
Prof. Dr. MARIA TOMOAIA-COTIȘEL**

Cluj-Napoca 2010

TABLE OF CONTENTS

Introduction.....	1
1. Methods and techniques of studying some orientated structures (biomembrane model) at interfaces.....	2
1.1. Surface tension and pressure.....	3
1.2. Langmuir-Blodgett Technique (LBT).....	9
1.3. Atomic Force Microscopy (AFM).....	15
1.4. References.....	32
2. Adsorption films (Gibbs) at fluid interfaces.....	35
2.1. Adsorption dynamics.....	35
2.2. Models –Experimental.....	36
2.2.1. Stearic Acid film at oil/water interface.....	41
2.2.2. Anesthetics films at oil/water interface.....	52
2.3. References.....	56
3. Langmuir films – lipid membrane models.....	57
3.1. Stearic Acid compression isotherms.....	57
3.2. Dipalmitoyl phosphatidylcholine compression isotherms.....	59
3.3. Dimyristoyl phosphatidylcholine and Cholesterol compression isotherms	62
3.4. Langmuir films phase structures	65
3.5. Subphase effects on Langmuir films.....	69
3.6. Modeling the interactions in the fatty acids films	72
3.7. References.....	79
4. Theoretical mathematical models. Oriented structures (biomembranes).....	82
4.1. Interpolation using spline functions of compression isotherms.....	82
4.1.1. Phase transitions in biomembranes	84
4.1.2. Surface compressibility of fatty acid films.....	87
4.2. Extended cubic spline functions modeling of compression isotherms.....	90
4.3. References.....	101
5. Langmuir-Blodgett membranes (films).Atomic force microscope observations..	106
5.1. Bioengineering and optimization of Langmuir-Blodgett films transfer conditions.....	106
5.1.1. Langmuir-Blodgett films transfer speed.....	107
5.1.2. Langmuir-Blodgett films transfer pressure.....	107
5.2. Subphase effects on lipid Langmuir-Blodgett films.....	108
5.2.1. Procaine influence	108
5.2.2. Deferoxamine influence	121
5.3. Langmuir-Blodgett monolayer membrane structures.....	127
5.4. Membranes collapse structures at air-water interface.....	136
5.5. Lipid monolayers membranes of dimyristoyl phosphatidyl choline and cholesterol	143
5.6. Collagen proteic membranes.....	146
5.6.1. AFM observations of molecular associations of collagen.....	146
5.6.2. AFM observations of anti-cancer drugs.....	151
5.6.3. Collagen membranes morphology in presence of anti-cancer drugs....	153
5.7. References.....	157
6. Biological membranes. AFM observations of erythrocytes.....	160
6.1. Microscopy observation of erythrocytes membrane.....	161
6.2. AFM observations of erythrocytes treated with procaine.....	183
6.3. AFM observations of erythrocytes treated with deferoxamine.....	195
6.4. References.....	213
7. Conclusions.....	216
8. General References.....	221
9. List of original publications.....	229

Key words: adsorption dynamics, monolayers, bilayers, surface pressure, surface potential, compression isotherms, Langmuir technique, surface compressibility, state equations, spline functions, LBT, AFM, fatty acids, lipids, cholesterol, collagen, anesthetics, anti-cancer drugs, erythrocytes, biomembrane.

ABREVIATIONS

AFM – atomic force microscopy
CHOL – cholesterol
CL – condensed liquid
COL – collagen
D – dibucaine
DFO – deferoxamine (desferal)
DPPC – dipalmitoyl phosphatidylcholine
DMPC – dimyristoyl phosphatidylcholine
DOX – doxorubicin
ECS – extended cubic spline
EL – expanded liquid
FLU – 5-fluorouracil
LBT – Langmuir – Blodgett technique
LA – linoleic acid
LPA – lipoic acid
OA – oleic acid
P – procaine
RMS – root mean square
S – solid
SA – stearic acid
SC – solid condensed
T – tetracaine

INTRODUCTION

The research and developments are taking place in chemistry and physics, chemical industry, biophysics, drug industry, involving knowledge of thermodynamic, kinetic and hydrodynamic processes that characterize thin films as lipid membranes and biomembrane models. These are of a great need in medicine, biology and pharmacy for new drug delivery systems and for the investigation of membranes in interaction with drugs with a high impact on the molecular mechanism of various diseases.

Modern surface science approaches have opened broad opportunities in different fields including fundamental concepts and theories on deciphering colloidal nanosystems containing surfactants, colloidal dispersions, colloidal electrolytes, foams, thin films, Langmuir films and model biomembrane.

There is an ongoing concern regarding monolayers since the beginnings of this investigation, interest motivated by the desire to understand the nature of interaction forces within oriented structures. Monolayers of fatty acids and phospholipids were examined mainly because they are accepted as membrane model systems and can offer a stable frame to investigate the interactions of various chemical compounds with the lipid membranes. The lipid systems are chemically well defined and accessible for investigation by different modern techniques becoming excellent models for the investigation of physical and chemical properties of biomembranes.

This thesis consists of six chapters followed by conclusions, general references and the list of original publications. The first chapter refers to the methods and techniques used to prepare and characterize the biomembrane models used in this scientific research. The original results are presented in five chapters and the main aspects studied are:

- Adsorption dynamics of the Gibbs films at liquid interfaces was explored using experimental measurements of dynamic interfacial pressures of high precision. To interpret the data, some theoretical models of adsorption kinetics were tested and a new diffusion controlled kinetic equation was proposed by coupling the Ward and Tordai diffusion equation with the van der Waals state equation of adsorbed layers.
- Insoluble Langmuir films of fatty acids and lipids were examined and characterized by compression isotherms and the best of mathematical models were selected to describe the behavior of these films at the air/water interface. In this respect, several mathematical curve fitting models were used and the surface compressibility was calculated; the extended cubic spline functions proved to approximate the experimental isotherms with considerable precision.
- Modern techniques, such as Langmuir-Blodgett technique combined with atomic force microscopy observations, were used to study the behavior of films of fatty acids, lipids and proteins and for the modeling of the interactions of some chemicals (anesthetics, steroids, anticancer drugs) with lipids and proteins of the cell membrane. This investigation represents a pioneering work with large applications in medicine, biology and pharmacy.
- The nanostructure of erythrocyte membrane surface and its changes in the presence of drugs were evaluated by atomic force microscopy observations. Modeling of erythrocyte membrane interactions with drugs, such as procaine and deferoxamine, and the membrane nanostructure visualization were first done in our laboratories, and represent a pioneering work.

The understanding the biomolecules self-assembling processes at the fluid interfaces is essential for the description of structure and function of these biomolecules. To elucidate these interfacial structures we used state of the art techniques to obtain scientific data at the nanometric level. Atomic force microscopy (AFM) coupled with Langmuir-Blodgett technique (LBT) are unique and powerful because they allow investigation of individual molecules on both the surface of LB structures and on biological structures, such as erythrocytes membrane.

2. Adsorption films (Gibbs) at fluid interfaces

2.2. Models – Experimental

The adsorption dynamics of some biosurfactants, *e.g.*, local anesthetics, namely dibucaine and tetracaine, from aqueous solutions (pH 2) to benzene/water (pH 2) interface and a fatty acid, *e.g.*, stearic acid, from benzene to the benzene/water (pH 2) interface has been studied using pendant drop and ring methods. Measurements of the dynamic interfacial tension at different surfactant concentrations give information on the adsorption kinetics and on the structure of the adsorbed layer of biosurfactants at liquid interfaces.

The ratio of the adsorption and desorption rate constants (table 2.2.5) obtained independently from dynamic data seems reasonable for the investigated systems. The rate constants are in good agreement with the literature data [98-100] and with the molecular structure of the biosurfactants.

Table 2.2.5. Relative adsorption (k_1/Γ_∞) and desorption (k_2/Γ_∞) rate constants.

Biosurfactant	k_1/Γ_∞ , $\text{mol}^{-1}\text{dm}^3\text{min}^{-1}$	k_2/Γ_∞ , min^{-1}	k_1/k_2 , $\text{mol}^{-1}\text{dm}^3$
Dibucaine	7.25	0.159	45.6
Tetracaine	4.99	0.149	33.5
Stearic Acid	0.212	0.0392	5.4

where k_1 and k_2 are the rate constants for the adsorption and for the desorption process, respectively; Γ_∞ is the equilibrium adsorption at the saturation of the interface with biosurfactant molecules.

We have evidenced the effects of the bulk phase, where the biosurfactant is soluble, on its adsorption at the oil/water interface. Thus, it is found that the adsorption rate constant depends on the molecular structure of the biosurfactants and of the nature of the bulk phase where the surfactant is soluble. The kinetic constants are higher for anesthetics than the corresponding ones for SA. The k_1/k_2 ratio for the adsorption of dibucaine and tetracaine from the water phase at the benzene/water interface is also higher than that corresponding to the adsorption of stearic acid from benzene at the same oil/water interface.

This might be due to the large flexibility of the SA long molecule with saturated chain and a terminal carboxylic polar group that may form aggregates both in bulk benzene solutions and within the adsorbed layers of SA at the benzene/water interface. The reorientation of molecules and the formation of surface self-assemblies within the adsorbed monolayers can also explain, at least in part, the low diffusion coefficient of the stearic acid in the benzene phase.

Various diffusion controlled kinetic equations have been tested and a *new improved diffusion controlled kinetic equation* is proposed (eq. 2.2.28), based on the Ward and Tordai's diffusion equation [97] associated with a two dimensional state equation of van der Waals type [111-115] for the biosurfactant adsorbed monolayers at the benzene/water interface.

$$\Pi = a \left[\frac{\tau^{1/2}}{1 - b\tau^{1/2}} - c\tau^{3/4} \right] = a\varphi(\tau) \quad (2.2.28)$$

with parameters:

$$a = 2kT(c_0 - c_s) \left(\frac{Dt_m}{\pi} \right)^{1/2}, \quad b = 2A_0(c_0 - c_s) \left(\frac{Dt_m}{\pi} \right)^{1/2}, \quad c = \frac{2^{1/2}\alpha(c_0 - c_s)^{1/2}}{kT} \left(\frac{Dt_m}{\pi} \right)^{1/4}$$

where: Π is the interfacial pressure, A_0 is the monolayer own area, k is the Boltzmann constant, T is the absolute temperature, c_0 represents the surfactant bulk concentration far from the interface, c_s is the surfactant subsurface concentration, D is the diffusion coefficient, $\pi = 3.14$, τ is a variable ranging from zero to t , t_m is maximum time, and α is the interaction parameter.

Table 2.2.11 combined with **Table 2.2.15**. Parameters of Eq. (2.2.28) derived from our experimental dynamic adsorption data for the three biosurfactants at the benzene/water (pH 2) interface.

Biosurfactant	C_0 , mol/l	t_m , min	Π_m , mN/m	a	b	c	$(SD)_m$ mN/m
Dibucaine	0.001	15	8.2	13.84	0	0.407	0.0028
	0.005	15	15.5	31.87	0.0039	0.518	0.0029
	0.010	15	18.9	46.14	0	0.590	0.0014
Tetracaine	0.001	15	5.2	10.31	0.0697	0.571	0.0047
	0.005	15	8.7	20.10	0.0465	0.616	0.0025
	0.010	15	11.0	26.60	0	0.586	0.0028
Stearic Acid	0.001	90	4.5	11.78	0.0813	0.706	0.0060
	0.0018	90	6.4	15.62	0	0.590	0.0046
	0.0057	90	12.1	32.86	0.0039	0.635	0.0019
	0.012	90	15.6	44.50	0	0.649	0.0019
	0.018	90	18.1	53.76	0.0019	0.665	0.0022
	0.051	90	22.0	85.43	0.163	0.937	0.0054

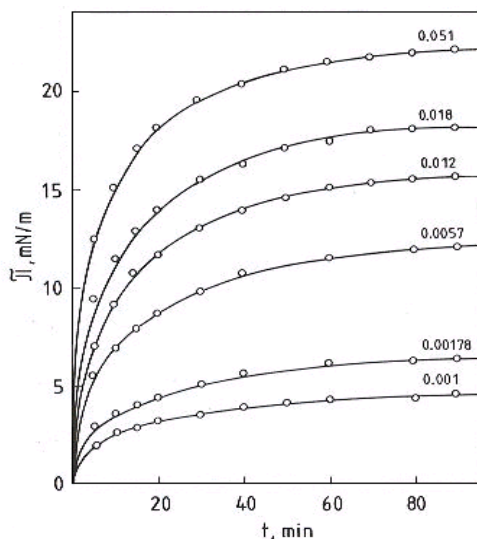


Fig. 2.2.3. Experimental dynamic interfacial pressure (Π in mN/m) of SA benzene solutions at the benzene/water (pH 2) interface as function of time (t , min). Figures indicate de SA bulk concentration C_0 in mole/L. Solid line calculated according to Eq. (2.2.28).

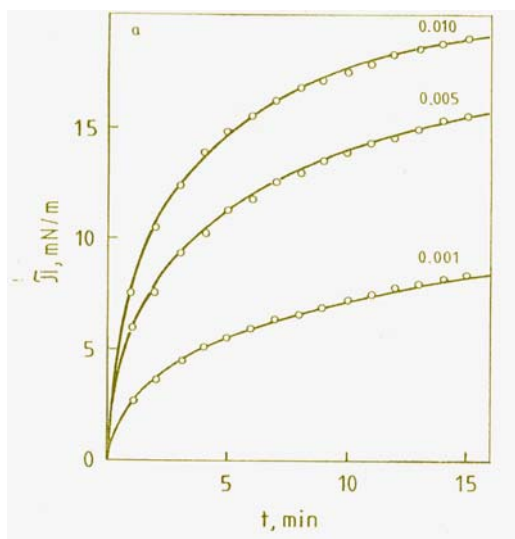


Fig. 2.2.12. Experimental dynamic interfacial pressure (Π in mN/m) of dibucaine aqueous solutions at the benzene/water (pH 2) interface as function of time (t , min). Figures indicate dibucaine bulk concentration C_0 in mole/L. Solid line calculated according to Eq. (2.2.28).

In Table 2.2.11 the parameters of Eq. (2.2.28) are given and they allow us to construct the theoretical Π versus t curves. These curves are given in Figs 2.2.3a, 2.2.12a and 2.2.13a as *full* curves.

Thus, it is clearly shown that Eq.(2.2.28) may describe very well the experimental Π versus t curves. Also, it allows the calculation of the diffusion coefficients, the subsurface concentrations and the interaction parameter α among biosurfactants molecules within the adsorbed monolayers at the benzene/water interface (Tables 2.2.12 and 2.2.16).

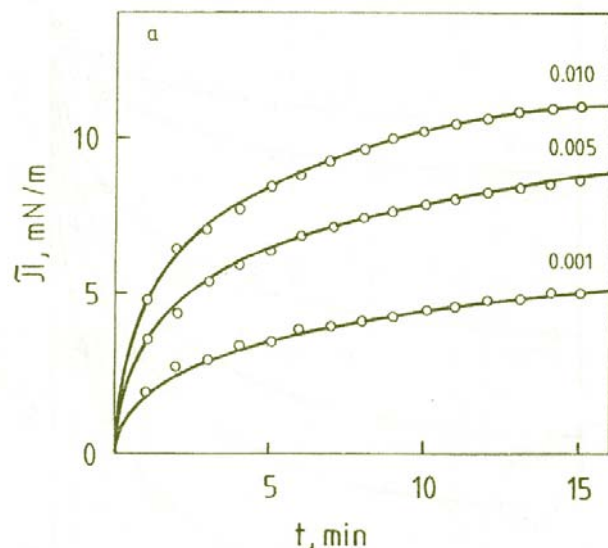


Fig.2.2.13. Experimental dynamic interfacial pressure (Π in mN/m) of tetracaine aqueous solutions at the benzene/water (pH 2) interface as function of time (t , min). Figures indicate tetracaine bulk concentration C_0 in mole/L. Solid line calculated according to Eq. (2.2.28).

Table 2.2.12 and 2.2.16. Diffusion coefficients, D and D_0 , subsurface concentrations C_s , and interaction parameters α

Biosurfactant	C_0 , mol/l	$D \cdot 10^{10}$, $\text{cm}^2 \text{s}^{-1}$	$D_0 \cdot 10^{10}$, $\text{cm}^2 \text{s}^{-1}$	C_s , mol/l	$*\alpha \cdot 10^{22}$, dyn cm^2
Dibucaine	0.001	2.840	2.84	0	8.90
	0.005	0.602		2.70	7.46
	0.010	0.316		6.67	7.07
Tetracaine	0.001	1.580	1.58	0	14.4
	0.005	0.240		3.05	11.2
	0.010	0.105		7.42	9.25
Stearic Acid	0.001	0.343	0.343	0	16.7
	0.0018	0.190		0.45	12.1
	0.0057	0.0821		2.91	9.02
	0.012	0.0840		8.22	7.92
	0.018	0.0220		13.4	7.38
	0.051	0.0069		43.7	8.24

* $\alpha \cdot 10^{28}$ mN m² in SI

Finally, the physical and chemical characterization of the biosurfactant monolayer adsorbed at the liquid interfaces is important and might have a great impact on many diverse phenomena, such as interfacial turbulence, foaming and wetting processes. Also, the dynamic behavior of biosurfactants plays a major role both in biological and biochemical processes as well as in technological ones.

3.Langmuir films – lipid membrane models

Characterization of compression isotherms, surface pressure (π) *versus* mean molecular area (A) of fatty acids, phospholipids and cholesterol films is essential to the study of many biological processes involving multicomponent systems.

3.1.Stearic Acid compression isotherms

Stearic acid is an example of an amphiphilic biocompound that is insoluble in water and self-assembles as a stable Langmuir monolayer at the air/water interface. Due to its high surface stability, SA is considered as a model compound suitable for nanolayers research [13-17].

Valuable informations on the molecular organization of SA in monolayers and collapse mechanism are obtained from compression isotherms [119].

From previous studies on the collapse mechanism of an insoluble Langmuir monolayer at the air/water interface theoretical models were developed [120-124]. The states of collapsing processes for an over-compressed Langmuir monolayer are shown in Fig. 3.1.2 [3].

Experimentally, the incipient collapse is often observed at a very reproducible collapse pressure, corresponding to a metastable equilibrium between the nanolayer and the undetectable freshly collapsed bulk phase [40, 125].

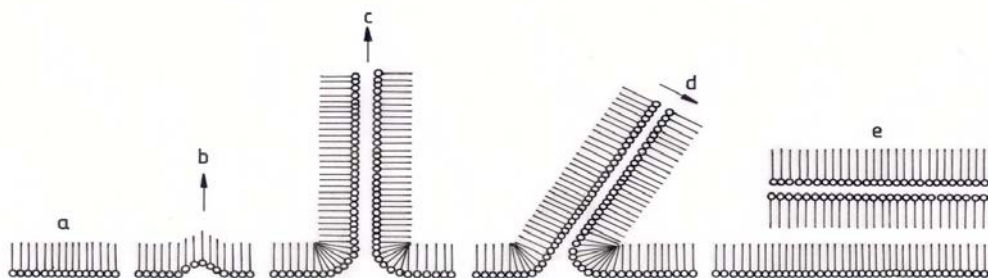


Fig.3.1.2. States of collapsing processes and collapsed structures obtained during the over compression of condensed SA monolayers. Arrows show the movement of molecules in different structures. The drawing are not at scale.

Theoretical studies of collapsing processes in SA monolayer [122] showed that by increasing the lateral surface pressure over incipient collapse pressure of SA monolayer, at incipient collapse SA monolayer existing in a two-dimensional condensed phase (Fig.3.1.2a), a buckling process might evolve in the plane of the monomolecular film (Fig. 3.1.2b) which entails film breaking and the formation of bilayers as vertical ridges (Fig. 3.1.2c) which can rise to the air phase. These ridges bend (Fig. 3.1.2d) and end up in breaking down over the remaining monomolecular film as a collapsed fragment and therefore, trilayers (Fig. 3.1.2e) may appear. Further, we will provide more detailed experimental evidence on collapse structures obtained in SA monolayers by using LB technique and AFM investigations [119].

The Langmuir monolayers of SA in the absence and in the presence of drugs at the air/water interface were studied. Compressions isotherms for pure SA monolayer and for SA monolayer in the presence of procaine: P (Fig. 3.4.3a) and deferoxamine: DFO (Fig.3.4.3b) were obtained for two different temperatures (*i.e.*, 20⁰C in Fig.3.4.3a and 22⁰C in Fig. 3.4.3b).

As a general behavior, one may observe that both isotherms of pure SA monolayers (Figs. 3.4.3a and b, curves 1) contain two linear portions corresponding to the LC and S states with a two-dimensional phase transition at a lateral surface pressure of about 26 mN/m.

In the presence of P (curve 2, Fig. 3.4.3a) or DFO (curve 2, Fig.3.4.3b) in the aqueous subphase the compression isotherms are moved to a larger molecular areas of SA showing the expansion of SA monolayers. For these compression isotherms, the surface characteristics of monolayers were determined and they are given in Table 3.4.1.

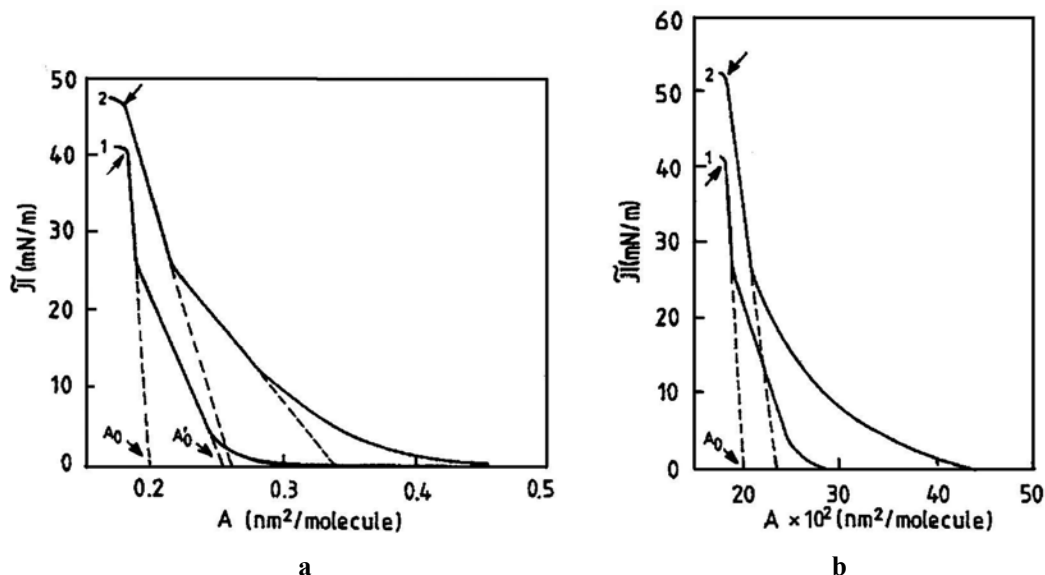


Fig. 3.4.3. a) – Compression isotherms for pure SA monolayer (curve 1) at the air/aqueous solution of pH 2 interface and for SA monolayer in the presence of 10^{-3} mole/dm³ P in the aqueous subphase (curve 2). Dashed lines indicate limiting areas for SA molecule in CL (A_0') and in S phase (A_0). Arrows at high surface pressures indicate the incipient collapse of SA. **b)** – Compression isotherms for pure SA monolayer (curve 1) at the air/aqueous solutions of pH 2 interface and for SA monolayer in the presence of 10^{-6} mole/dm³ DFO in the aqueous subphase (curve 2). Symbols as in Fig.3.4.3a.

Table 3.4.1. Surface characteristics of Langmuir monolayers of SA on aqueous subphases of pH 2 in the absence and in the presence of P (10^{-3} mole/dm³) or DFO (10^{-6} mole/dm³). The mean area values (A_0' , A_0 and A_c) are given in nm²/molecule of SA.

Monolayer	A_0' (nm ²)	A_0 (nm ²)	A_c (nm ²)	π_c (mN/m)	
				incipient	advanced
AS	0.255	0.200	0.180	40.8	(45.0)
AS and P	0.340	0.260	0.175	46.7	(50.9)
AS and DFO	0.320	0.230	0.180	52.5	(56.7)

The incipient collapse pressure (π_c) is the highest surface pressure to which a Langmuir monolayer can be compressed at the air/water interface [13,15,40,133] and corresponds to the sudden slope change observed on the isotherms at high surface pressures (see, arrows at high pressure on Fig. 3.4.3). The corresponding mean molecular areas are the collapse areas (A_c) and they are also given in Table 3.4.1.

It is important to emphasize that we have chosen these two very different concentrations of drugs, because for these conditions P and DFO have an important (see, π_c in Table 3.4.1) and comparable effect (see, A_0 and A_c values) on the phase behavior of SA monolayers. However, the collapse pressure increment (about 11.7 mN/m) due to DFO is almost double than for procaine (approx. 5.9 mN/m). The increased stability of SA monolayers in the presence of DFO reflects stronger specific interaction between SA and DFO, due to the flexibility of the large DFO molecule and its ability to make stable surface complexes with SA molecules [34] through hydrogen bonds. The SA and DFO molecules form a more ordered hydrogen bonding network within this monolayer compared with the mixed monolayers of SA and P.

3.2. DPPC compression isotherms

The compression isotherm of pure DPPC monolayer, spread at the air/water interface is given in Fig. 3.2.4, curve 1. At about 8 mN/m, the DPPC monolayer exhibits a two-dimensional phase transition [42], from EL to CL, shown on the compression isotherm (Fig.3.2.4, curve 1) by a sharp break in the isotherm slope. At this main transition, two phases EL and CL coexist in the DPPC monolayer.

The linear portion of high lateral surface pressures corresponds to the CL state, followed by an intermediary liquid corresponding to intermediate surface pressures (between 8 and 20mN/m) and by an EL state under 8 mN/m [59]. In the presence of

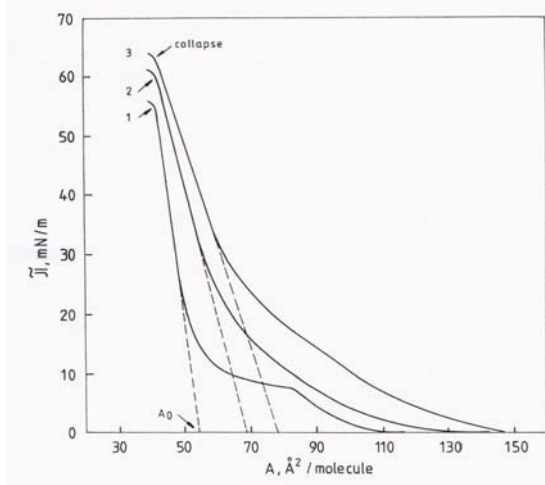


Fig. 3.2.4. Compression isotherms at the air/ water interface for pure DPPC monolayer (curve 1) and for DPPC monolayer in the presence of DFO (10^{-6} mole/dm³, curve 2) in the aqueous phase, or of P (10^{-3} mole/dm³, curve 3), at 20 °C. Dashed lines indicate the limiting areas for DPPC molecule (A_0) in CL state. Arrows at high surface pressures indicate the incipient collapse state of monolayers.

deferoxamine (10^{-6} mole dm⁻³; curve 2, Fig.3.2.4) or procaine (10^{-3} mole dm⁻³; curve 3, Fig.3.2.4.) in the aqueous subphase the compression isotherms are moved to larger molecular areas of DPPC showing the drug expanding effect on DPPC monolayers.

From compression isotherms, the surface properties of DPPC monolayers were determined and they are given in Table 3.4.2. For instance, the A_0 is the limiting molecular area for the CL state of DPPC monolayers in the absence or in the presence of drugs. These A_0 values are obtained by extrapolation at π equals zero of the linear portion of the isotherms recorded at high lateral pressures (Fig. 3.2.4). By comparing the A_0 values (Table 3.4.2.) it is evidenced the drug expansion effect on the CL state of DPPC monolayers.

Table 3.4.2. Surface characteristics of DPPC monolayers in the absence and in the presence of P (10^{-3} mole dm⁻³) or DFO (10^{-6} mole dm⁻³). The mean area values (A_0 , and A_c) are given in Å²/molecule of DPPC. The π_c values correspond to the monolayer collapse.

Monolayer	A_0 (Å ²)	A_c (Å ²)	π_c (mN/m)	
			incipient	(advanced)
DPPC	54	42	55	-
DPPC and DFO	69	42	59	(70)
DPPC and P	78	42	63	(70)

As can be seen, the A_c values are constant. This situation can be correlated with the squeezing out of penetrated drugs from mixed DPPC and drug monolayers near their incipient collapse.

The increased stability of DPPC monolayers in presence of P or DFO reflects stronger specific interactions between these biocompounds, due to their ability to make stable self assembled supramolecular associations primarily through hydrogen bonds and electrostatic interactions [90, 139, 221].

3.3. DMPC and CHOL compression isotherms

The phase behaviour of DMPC and CHOL monolayers at the air/water interface was investigated by surface pressure and surface potential measurements using Langmuir technique. These two biocompounds are examined, namely DMPC and CHOL, both in pure state and in mixture DMPC:CHOL (4:1) for a well defined molar fraction of 0.8 in DMPC.

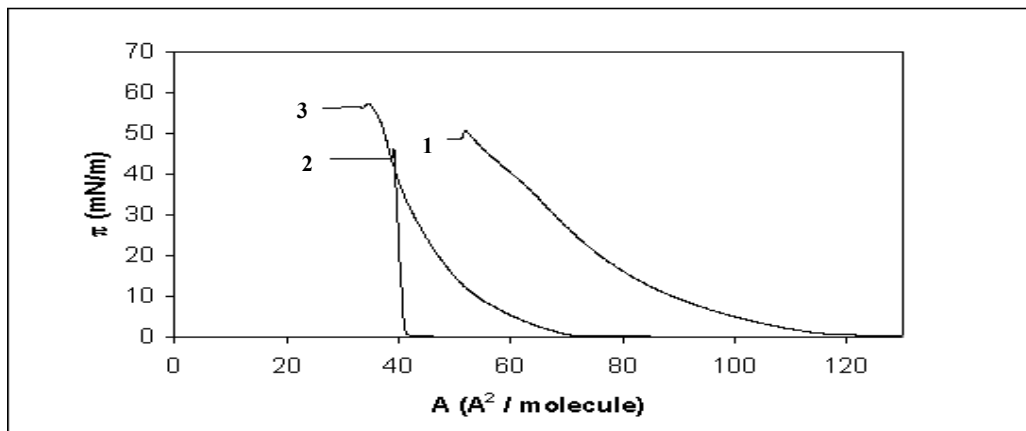


Fig. 3.3.3. Compression isotherms, surface pressure (π) versus mean molecular area (A), at the air/water interface for the following Langmuir monolayers: DMPC (curve 1), CHO (2) and the DMPC:CHO mixture with a DMPC molar fraction of 0.8 (3). Water subphase of pH 5.6 at 20 °C.

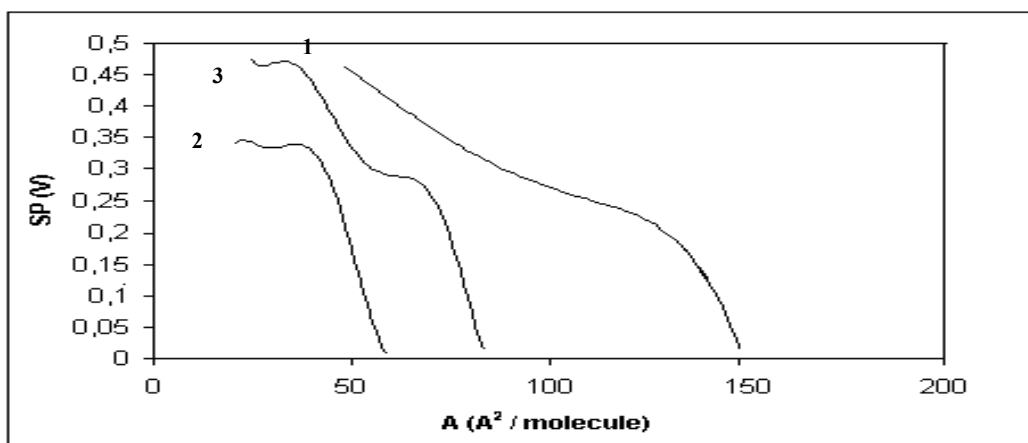


Fig.3.3.4. Surface potential (SP) versus mean molecular area (A) of the following monolayers: DMPC (curve 1); CHO (2); DMPC:CHO mixture with a DMPC molar fraction of 0.8 (3). Experimental conditions as in Fig.3.3.3.

Figure 3.3.3 shows the compression isotherms for DMPC (curve 1), CHOL (curve 2) and for their mixture DMPC:CHOL in the chosen (4:1) molar ratio (curve 3). As a general behavior, one may observe that the DMPC monolayer becomes more condensed in the presence of CHOL. This behavior is further illustrated in Table 3.3.1, where the area per molecule for a closely packed monolayer (extrapolated to zero pressure) noted A_0 is shown to strongly decrease in the presence of CHOL. The overall appearance of the isotherm for the mixture (curve 3) remains rather similar with the DMPC isotherm (curve 1) particularly for low surface pressures. The collapse pressure of the mixture of DMPC:CHOL is highly increased (53 mN/m) when compared with the collapse pressure of the pure biocompounds, namely CHOL(45 mN/m) and DMPC (50 mN/m) (Table 3.3.1).

The experimental findings indicate that DMPC monolayer remains in the liquid state up to its collapse (see, surface compressional moduli: C_s^{-1} values, given in Table 3.3.1). In the case of CHOL, its pure monolayer is in a solid state, with very low lateral compressibility [43, 96]. As expected for high stability of the mixed systems, the collapse pressure of mixed DMPC:CHOL monolayer is shifted to higher collapse pressures than for the pure biocompounds [151,152].

The molecular areas (A_0 and A_c , Table 3.3.1) were determined from isotherms given in Fig. 3.3.3. The A_0 values support the miscibility of DMPC and CHO at this molar ratio (4:1) with negative deviations from the area additivity rule. This situation is found for a large interval of moderately high surface pressures. Interestingly, the mean molecular area at the collapse of the DMPC:CHOL (4:1) mixture is shifted completely towards the collapse area of CHOL in pure state (see Table 3.3.1) as shown for mixed DMPC:CHOL (7:3) monolayers ([150]). Therefore, the close-packed mixed monolayer presents the highest collapse pressure recorded for these biocompounds and it represents a strong evidence that both compounds are miscible within the two-dimensional structure, that is thermodynamically stable. The stabilization of the mixed DMPC:CHOL (4:1) monolayer is probably due to associative interactions established between these biocompounds.

Table 3.3.1. Surface characteristics of the following monolayers: DMPC, CHO, and the DMPC:CHO (4:1) mixture at the air/water interface (see Figs. 3.3.3 and 3.3.4).

Monolayer	State	A_0	A_c	π_c , mN/m	C_s^{-1} , mN/m	$A_{\Delta v}$	ΔV , mV
DMPC	LE	90±2	53±2	50±2	87	190±5	450±10
CHOL	SC	40±1	39±2	45±1	1074	57±5	340±10
DMPC:CHOL (4:1)	LC	48±1	37±2	53±1	186	88±3	470±5

A_0 , A_c and $A_{\Delta v}$ are given in $\text{\AA}^2/\text{molec.}$

These results (Fig. 3.3.3) are also consistent with surface potential measurements (Fig. 3.3.4). The CHOL biomolecules are incorporated into the DMPC monolayer and change the surface potential. Fig. 3.3.4 shows that the surface potential curve for the mixture (3) is placed between the curves for the pure monolayers, similarly with the results given in Fig. 3.3.3. The maximum surface potentials reached are displayed in Table 3.3.1. Generally, the DMPC monolayers become more condensed in the presence of CHOL (Fig. 3.3.3) and the critical area for the increase in the surface potential (noted, $A_{\Delta v}$, given in Table 3.3.1; for simplicity not shown on curves in Fig.3.3.4) is also significantly decreased against the corresponding value of pure DMPC monolayer. This critical area is related to the mixed monolayer structure which causes the sharp decrease of the effective dielectric constant at the air/water interface.

The change in surface potential of mixed monolayer due to the incorporation of CHOL can be attributed to specific interactions among these biocompounds, which are neutral at the working pH (5.6) of all experiments. The contribution from the CHOL incorporated into the DMPC monolayers in terms of the dipole moment appears to be associated with the orientation of the polar groups of both components and with the specific interactions among them within the mixed DMPC:CHOL (4:1) monolayer.

The increased stability of DMPC monolayers in presence of CHOL reflects stronger specific interactions between these biocompounds, due to their ability to make stable self assembled supramolecular associations primarily through hydrogen bonds and hydrophobic interactions [201].

3.6. Modeling the interactions in the fatty acids films

Many attempts have been made to give a mathematical description of the compression isotherms recorded for soluble and insoluble monolayers at the air/liquid interface [104-106]. The regression techniques, using an empirical curve fitting approach, select empirical models characterized by a particular equation derived as two-dimensional van der Waals-type equations. These methods provide parameters that allow the accurate description of the compression isotherms particularly for low surface pressures corresponding to liquid expanded state of monolayers. The parameters of the chosen equation are systematically varied to provide the best fit to the experimental isotherms.

A comparative study of compression isotherms of OA, LA and SA monolayers spread at the air/water interface on acidic solutions (pH=2) and the testing of an state equation using the triple minimization method was made.

The equation was obtained from the equality of the chemical potential of water in the subphase and in the monolayer, by presuming the latter to be a regular solution of surfactant molecules (head groups only) in water and by using a semiempirical expression for contribution of the hydrocarbon chains of the surfactant to the surface internal pressure. The new improved equation is of the following form:

$$\pi = - \left(\frac{\alpha}{A^{3/2}} + \frac{kT}{A_1} \ln x_1 + \frac{\beta_{12}}{A_1} x_2^2 \right) = -\pi_0 + \pi_h \quad (3.6.12)$$

In this expression π stands for surface pressure, A stands for mean molecular area, π_h stands for contribution of the interaction of the water molecules and polar head groups of the fatty acids in the monolayer (thought to be a regular solution); the surface pressure $\pi_0 = \alpha / A^{3/2}$ represents the cohesive surface pressure due to the chain-chain hydrophobic interactions (characterized by the interaction parameter α) in the air phase part of the monolayer. Since in the expanded monolayer these interactions lead to intermolecular attraction, α must be the positive value. The interaction parameter, β_{12} , is defined as:

$$\beta_{12} = z \left(\varepsilon_{12} - \frac{\varepsilon_{11} + \varepsilon_{22}}{2} \right)$$

where z stands for the number of contacts of a molecule in the monolayer with neighbouring molecules, ε_{11} , ε_{22} and ε_{12} stand for potential energy corresponding to the water/water, head group/head group and water/head group interactions, in the monolayer, respectively. Taking into account the structure of the water molecule and of head group COOH, negative values may be expected for β_{12} . In Eq. (3.6.12), x_1 and x_2 are the molar fractions of water and of the polar head groups, in the monolayer solution, respectively. A_1 means the cross-section area of the water molecules in the monolayer, k stands for Boltzmann constant and T is the absolute temperature. The molar fraction x_2 can be calculated as:

$$x_2 = \frac{A_1}{A - A_2 + A_1} \quad (3.6.13)$$

where A_2 stands for the cross-sectional area of the polar head group; A_1 has been approximated as $A_1 = (V^{2/3})/N_A \cong 0.1 \text{ nm}^2/\text{molecule}$, where V and N_A stand for the molar volume of liquid water and for Avogadro's constant, respectively.

The parameters of Eq. (3.6.12), derived from the experimental compression isotherms of the fatty acid monolayers by means of triple minimization, are presented in Table 3.6.1.

Table 3.6.1. Parameters of the state equation (3.6.12) derived for the fatty acids studied ($\pi \leq 7 \text{ mN/m}$). Δ is the standard deviation of the experimental π values from the theoretical ones.

Surfactant	$A_2, \text{ nm}^2/\text{molec.}$	$\alpha \times 10^{30}, \text{ Nm}^2$	$\beta_{12} \times 10^{20}, \text{ Nm}$	$\Delta, \text{ mN/m}$
OA	0.225	7.714	-1.507	0.087
LA	0.265	6.932	-1.150	0.073
SA	0.207	2.593	+0.513	0.150

Inspection of table 3.6.1 shows that Eq.(3.6.12) describes very well the compression isotherms, especially with unsaturated fatty acids; and for these the standard deviation Δ is less than the experimental errors π measurements. The derived A_2 values seem to be quite realistic and characterize indeed the carboxyl head group. The increase of A_2 in the order $\text{SA} < \text{OA} < \text{LA}$ is not surprising, since at a given π value the monolayers have their molecular areas increasing in the same order, which might entail a modification in the head group conformation.

Concerning the β_{12} values obtained, they seem to be quite reasonable in the case of OA and LA, in both cases expressing strong attraction between the COOH group and water molecules, although their numerical values differ from each other.

The α values obtained for OA and LA are also very reasonable. They express strong hydrophobic interactions between the hydrocarbon chains, these interactions being stronger with OA as compared to LA, in good agreement with the higher collapse pressure of the former as compared to the latter.

All these results show that Eq. (3.6.12) gives a very good description of π versus A isotherms of OA and LA, up to $\pi = 7 \text{ mN/m}$, (see Fig. 3.6.4) yielding very reasonable A_2 , β_{12} and α values. Reversely, in the case of SA, the description is rather poor, Δ depassing experimental errors, and although Eq. (3.6.12) yields a reasonable A_2 value, the interaction parameters derived are rather unrealistic.

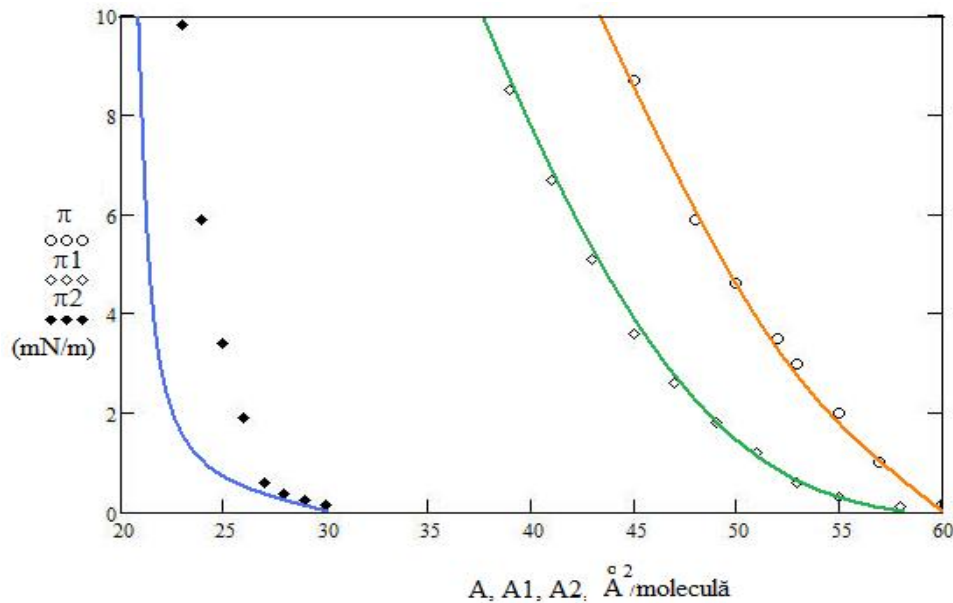


Fig.3.6.4. Experimental pairs π - A (for OA); π_1 - A_1 (for LA); π_2 - A_2 (for SA) and theoretical curves calculated with Eq.3.6.12 and parameters from Table 3.6.1.

One may conclude that Eq. (3.6.12) is a very good state equation for liquid expanded monolayers of fatty acids, but it cannot be applied to liquid condensed monolayers of saturated fatty acids [107].

4. Theoretical mathematical models. Oriented structures (biomembranes)

4.2. Extended cubic spline functions modeling of compression isotherms

The objective of this chapter is to perform a numerical analysis of compression isotherms of fatty acids using the experimental data of molecular area (A) *versus* surface pressure (π) of LA, OA and SA films. The mathematical method considers the use of the extended cubic spline functions and the method of least squares fitting. This method use the spline function interpolation, where the experimental curve is constructed from a series of curved segments which are joined together to form a smooth complete curve passing through the experimental points [180-182, 188].

MATHCAD 13 software was used to develop iterative calculations program by the method of least squares fitting with stepwise cubic polynomial of class C^1 , *i.e.* polynomial continuous together with its first derivative, also called, extended cubic spline function (ECS). This program was used to modeling the compression isotherms of fatty acids and to calculate the surface compressibility (C_s) of monolayers with a considerable precision from the spreading to the colapse of monolayers.

It is a known fact that a phase transition can be pointed aut by means of the surface compressibility values [13, 189-191], which depend on the physical state of the monomolecular films, being greater for more expanded monolayers. In determining the phase transformations usually the Ehrenfest criterion is used [195], which says that a phase change is of order m if the Gibbs free energy (G) partial derivative of the same order with respect to one of its variables shows a discontinuity at a given temperature while the lower order derivatives are continuous.

The first order derivative of G function with respect to π , assuming all the other state variables to be constant (namely, absolute temperature T and external pressure p) is given by:

$$\left(\frac{\partial G}{\partial \pi}\right)_{T,p} = A \quad (4.2.11)$$

where A stands for the mean molecular area of the chosen surfactant in the monolayer. Therefore, a discontinuity in area values at a constant surface pressure characterizes a transition of first order. By considering, further, the following relations:

$$\left(\frac{\partial A}{\partial \pi}\right)_{T,p} = \left(\frac{\partial^2 G}{\partial \pi^2}\right)_{T,p} \quad (4.2.12)$$

and

$$C_s = -\frac{1}{A} \left(\frac{\partial A}{\partial \pi}\right)_{T,p} \quad (4.1.1)$$

one infers that a discontinuity in C_s (expressed in m/mN) values can be taken as a discontinuity in the second order derivative G in relation with π , when A is a continuous function.

Results of computer software that model the compression isotherms and the compressibility coefficients for fatty acids with ECS functions and least squares fitting method are illustrated in Figures 4.2.7 – 4.2.12.

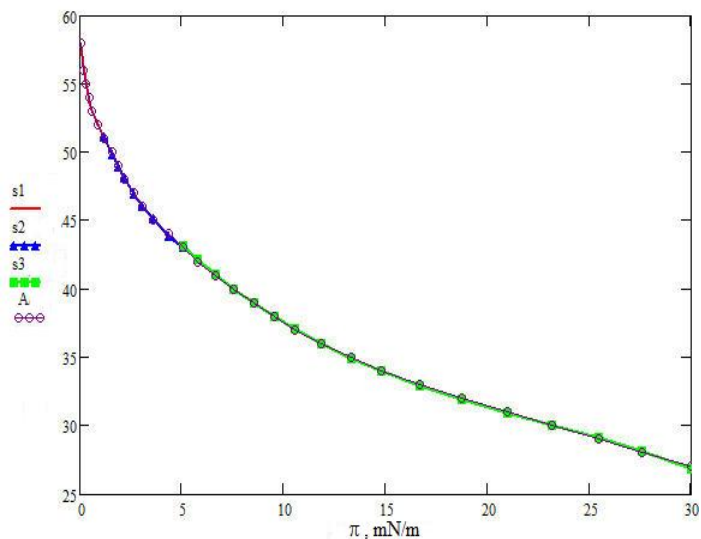


Fig. 4.2.7. Experimental data A versus π and extended spline functions (s1-s3) calculated with the method of least squares for OA, the second iteration. Average molecular areas are given in $\text{\AA}^2/\text{molecule}$.

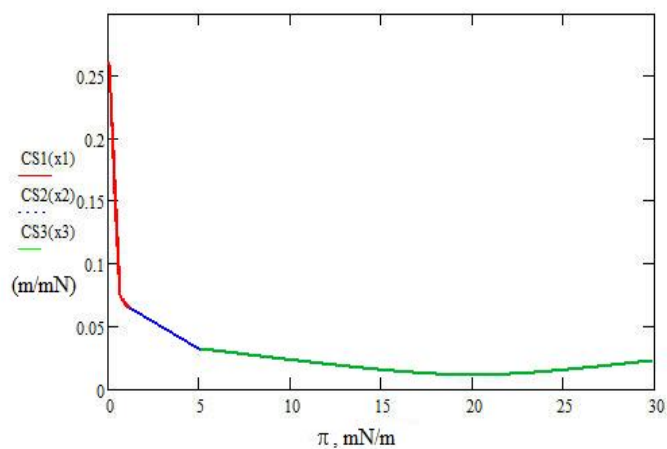


Fig. 4.2.8. Surface compressibility (CS) versus π calculated by derivation of ECS functions for OA.

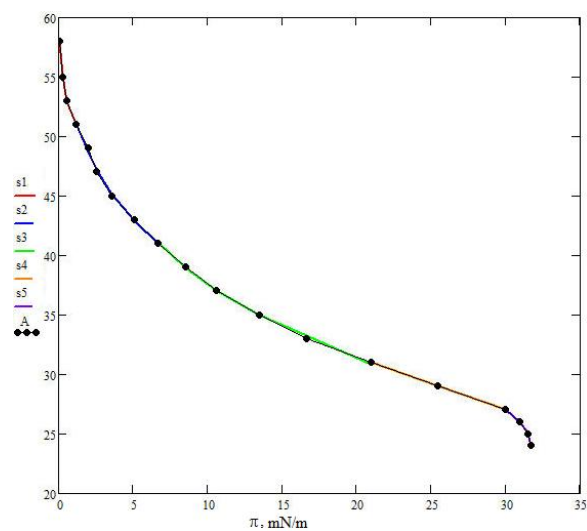


Fig. 4.2.9. Experimental data A versus π and ECS (s1-s5) calculated for LA, the fourth iteration. Average molecular areas are given in $\text{\AA}^2/\text{molecule}$.

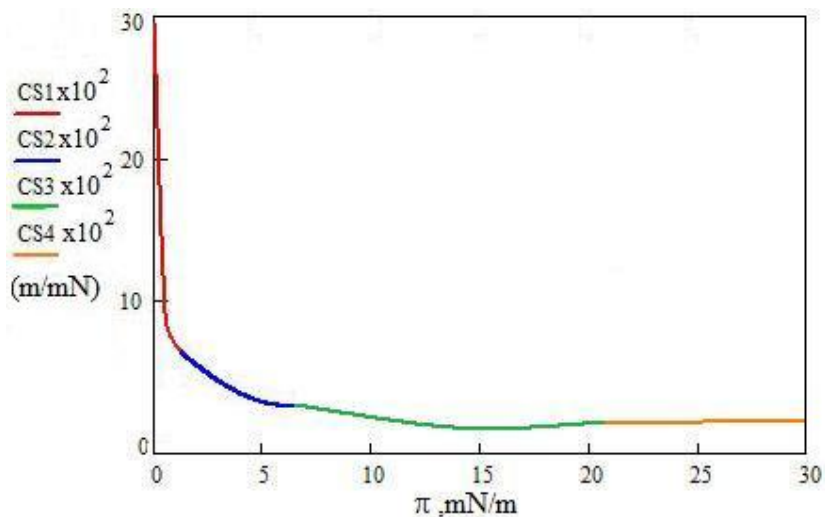


Fig. 4.2.10. Surface compressibility (CS) *versus* π calculated by derivation of ECS functions for LA.

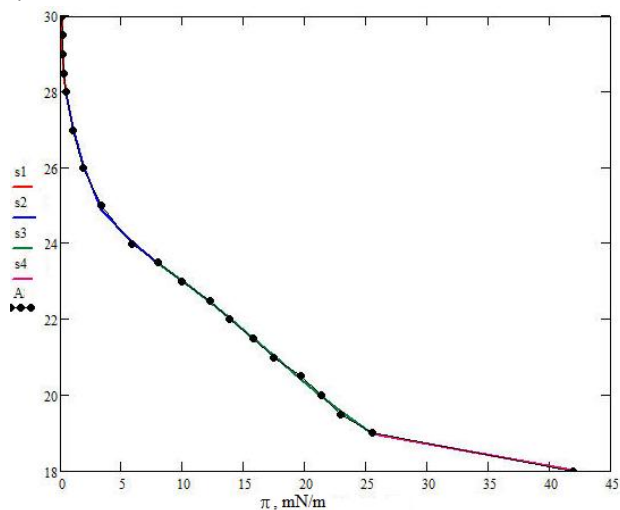


Fig. 4.2.11. Experimental data A *versus* π and ECS (s1-s4) calculated for SA, the third iteration. Average molecular areas are given in $\text{\AA}^2/\text{molecule}$.

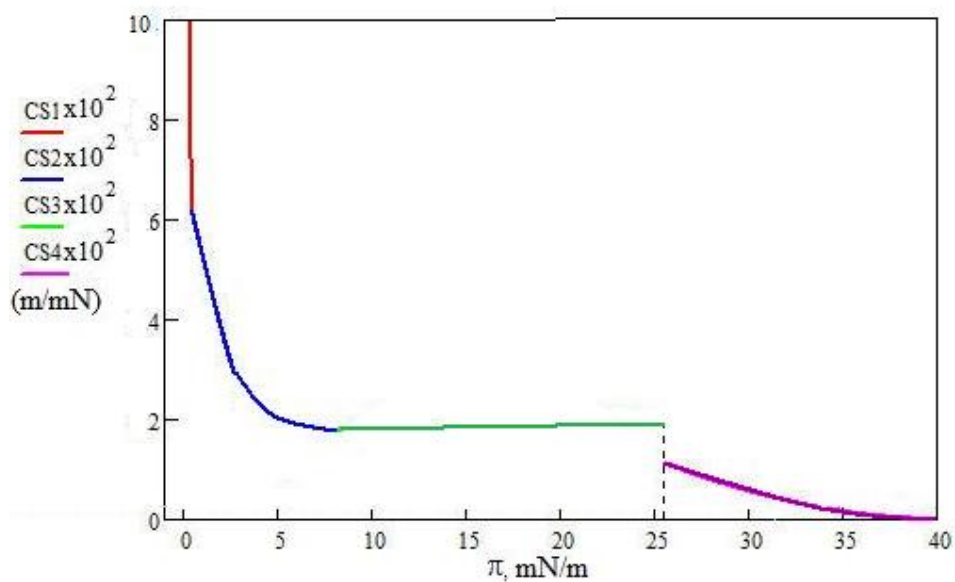


Fig. 4.2.12. Surface compressibility (CS1(x1)-CS4(x4)) *versus* π calculated by derivation of ECS functions for SA.

As seen from Figs. 4.2.7, 4.2.9 and 4.2.11 the method of least squares fitting with stepwise ECS functions form a smooth complete curve passing through the experimental points of compression isotherms of fatty acids.

Surface compressibility factors calculated by derivation of cubic polynomials ECS functions are realistic and close to the experimental values calculated from compression isotherms of fatty acids studied (Figs. 4.2.8, 4.2.10 and 4.2.12).

As seen from Figure 4.2.12 at the surface pressure of 26 mN/m of stearic acid there is a discontinuity of first order derivatives of ECS functions, so there is a second order phase transition from LC to S in the film AS, result is consistent with literature data [107, 188-191].

5. Langmuir-Blodgett membranes (films). Atomic force microscope observations

Atomic force microscopy (AFM) is a novel high-resolution surface imaging technique for nano-meter scale size structures and it is used for the visualization of different phases arranged in nanolayers, for structure investigation and size analysis of supramolecular aggregates [33,34,36,92,135-136]. AFM operates by measuring the forces acting between a probe (also called tip) attached to a cantilever and the LB film, which is called usual the LB sample. It is important to mention that in the tapping mode the AFM technique presents a specific advantage, such as the tip does not touch the LB sample and consequently the surface of the sample is not damaged. Moreover, the local chemical reactions on the LB film surface are not expected as a result of the interaction forces between the tip and the atoms of the LB film. The sensitivity of AFM measurements is very high and accurate information on the surface morphology at the molecular level is obtained.

5.2. Subphase effects on lipid Langmuir-Blodgett films

5.2.1. Procaine influence

Investigation of the surface morphology and domain structure of the LB sample of SA and DPPC in presence of procaine (P) were conducted in the tapping mode on a research AFM system with a 90 x 90(x-y) μm scanner and non-contact conical shaped tips of silicon nitride coated with aluminium. The tip was on a cantilever with a resonant frequency in the range of 200-300 Hz and with a spring constant of 17.5 N/m.

It was examined the influence of the surface pressure on the morphology of LB films of SA and DPPC in the presence of P (10^{-3}M) (Figs. 5.2.2, 5.2.9) [48, 49].

The AFM images of mixed SA and P films reveal their self-assembled association into less aggregated particles at advanced collapse state. Procaine leads to a more homogeneous phase in mixed LB films with SA particularly at high lateral pressure.

The AFM images indicate that the mixed DPPC and P films are not homogeneous at low surface pressure, which is plausible taking into account the different molecular length of the two molecules, DPPC and P, and their orientation at low pressures (Fig. 5.2.9)[15,17,42]. However, by increasing the surface pressures, AFM images indicate an increased cohesion among molecules reflected also in topographic profiles.

Therefore, it is evidenced the persistence of monolayer CL domains at very high surface lateral pressures in mixed DPPC and P films at advanced collapse state. The width of domains is up to 1.5 μm and corresponds to supramolecular aggregates, probably, made up from well oriented DPPC and P molecules primarily through hydrogen bonds and electrostatic interactions [60].

In conclusion, procaine stabilized SA and DPPC films at high lateral surface pressures. The drug distribution throughout the lipid membranes is useful to better understand the mechanism of anesthesia.

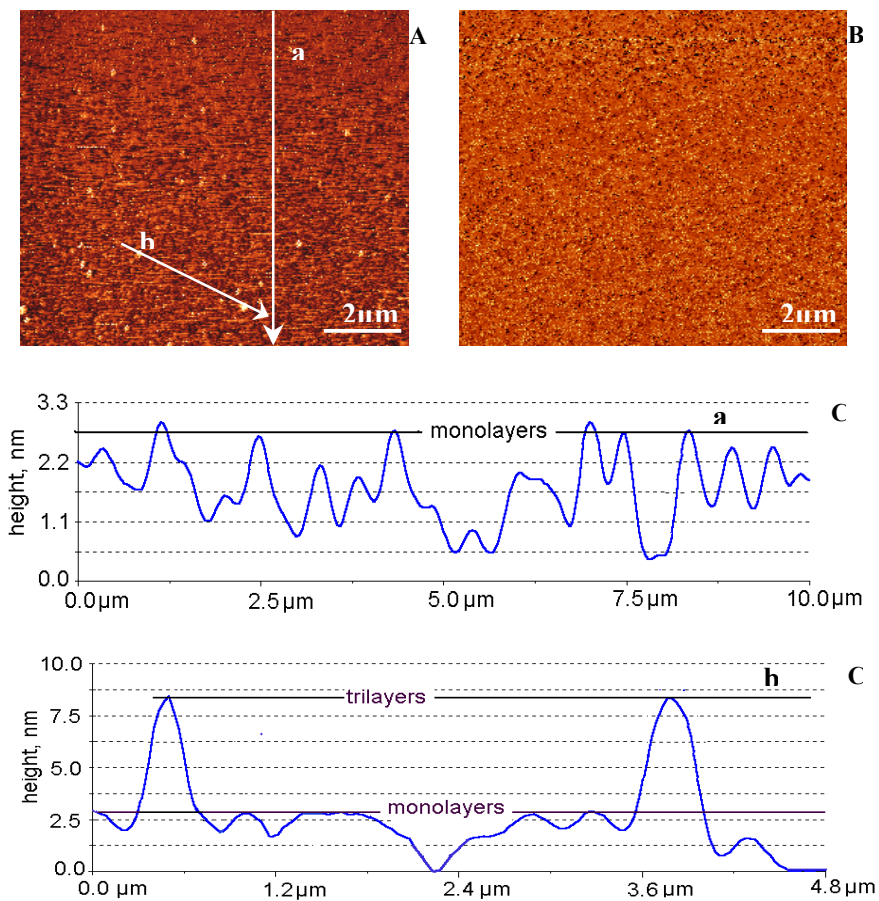


Fig.5.2.2. – 2D topographic (panel A) and phase (B) AFM images of LB films of SA transferred on glass at advanced collapse state (lateral surface pressure of 50.9 mN/m) in the presence of 10^{-3} mole/dm³ P in the aqueous subphase. Panel C – cross section profile; part a along the arrow a in Fig.5.2.2A; part b along the arrow b in

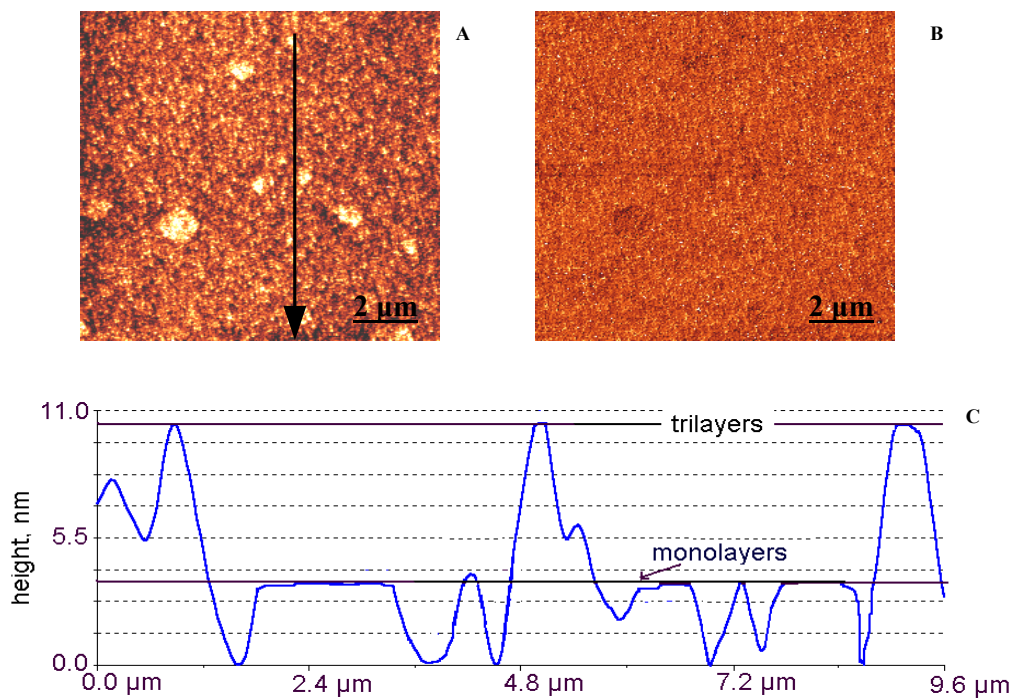


Fig. 5.2.9. The 2D topographic image (panel A) and phase image (panel B) and section profile (panel C) along the line (panel A) images for mixed LB films of DPPC and P vertically transferred at advanced collapse state (lateral surface pressure of 70 mN/m).

5.2.2. Deferoxamine influence

The LB film morphology of SA in the presence of DFO shows a homogeneous structure at low lateral surface pressures. The LB surface structure at advanced collapse is dominated by irregular aggregates consisting of solid large striations well packed, probably formed by surface complexes of SA and DFO strongly aggregated due to the electrostatic interactions and hydrogen bonding network resulting in big particles with three layered structure of about 1.5 μm average size, with height between 8.7 and 9.1 nm. These supramolecular self-assemblies are found in equilibrium with large monolayer domains of average size between 3.0 and 3.4 nm (Fig. 5.2.13) [49, 60,137].

The high stability of the large condensed domains (with the width up to 2.5 μm), identified in mixed DPPC and DFO films at advanced collapse, might indicate that the flexible DFO molecules are differently oriented than the DPPC molecules, and probably they are horizontally oriented beneath the DPPC monolayer. This interfacial orientation can facilitate the self-assembled molecular associations and, thus, it can stabilize the condensed monolayer domains (Fig. 5.2.16).

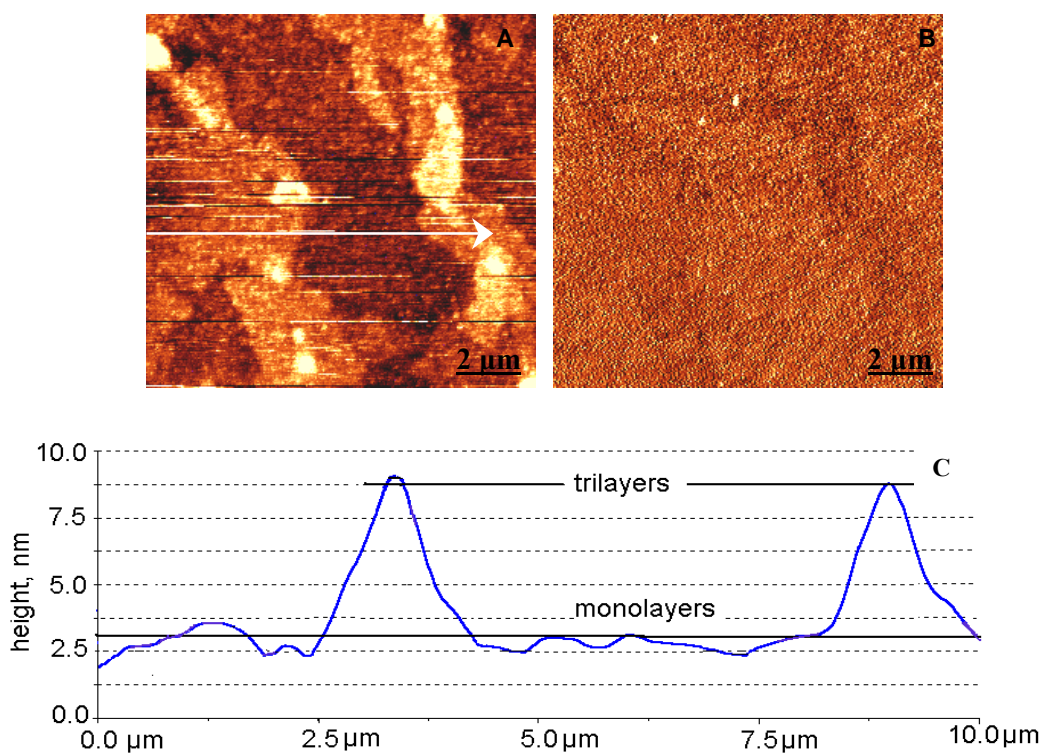


Fig. 5.2.13. The 2D topographic (panel A), phase image (panel B) and section profile (panel C) along the line (panel A) AFM images for mixed LB films of SA and DFO transferred on glass at advanced collapse state (lateral surface pressure of 56.7 mN/m) for 10^{-6} mole/dm³ DFO in aqueous subphase.

On the basis of different morphologies shown by AFM images both the formation of supramolecular self-assemblies and aggregates and their aligning process are probably a result of many kinds of interactions. These may include the interaction among lipid molecules and between lipids and drug molecules in addition to the interaction between the underlying substrate and the film forming molecules. The collective effect of these interactions might lead to the formation and alignment of various ordered structure, which can have a physiologic role *in vivo*.

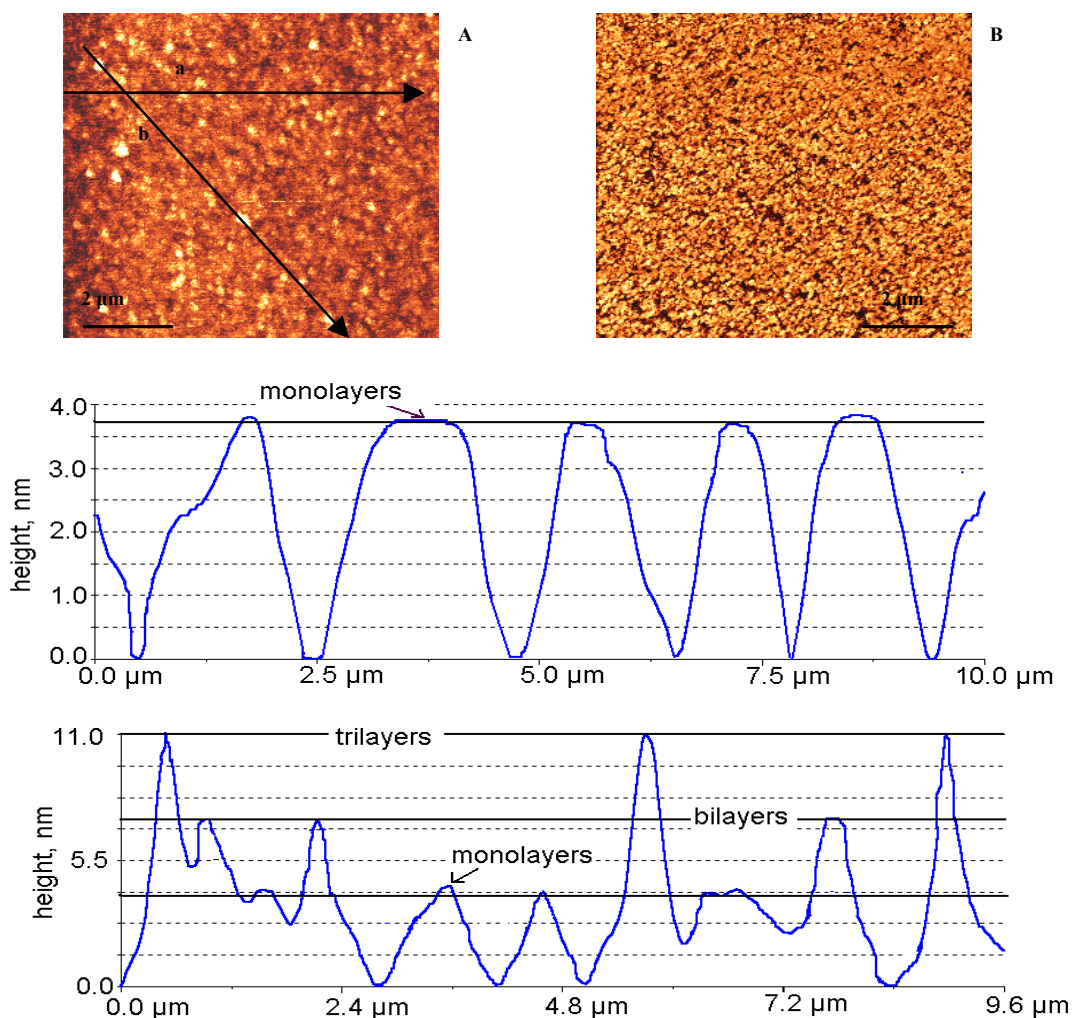


Fig. 5.2.16. The 2D topographic (panel A), phase (panel B) AFM images, section profile (panel C) along the lines (panel A) for mixed LB films of DPPC and DFO (10^{-6} mole/dm³) vertically transferred at advances collapse state (70 mN/m).

The studies have shown a long-term stability of LB films, transferred on different solid substrates from their Langmuir monolayers at the air/aqueous solution interface, as observed by the AFM images of these LB films, taken several days after transfer and repeated several months up to one year. The high stability of both LB films and Langmuir monolayers of these biocompounds would be useful in various applications for medicine, pharmacy and biology [25, 48, 49, 60, 137, 198].

5.5. Lipid monolayers membranes of dimyristoyl phosphatidyl choline and cholesterol (DMPC and CHOL)

AFM coupled with the Langmuir-Blodgett technique gives valuable information on the two-dimensional nanostructures of both pure DMPC monolayers and binary mixtures of DMPC with CHOL. The AFM images were obtained on LB films transferred on mica at two lateral surface pressures, namely 10 mN/m and 20 mN/m. The AFM images at several magnification for the DMPC:CHOL (4:1) mixture indicate that the mixed films are rather homogeneous at both surface pressure with a very low roughness [146, 147].

The changes in the nanostructure of DMPC in the presence of CHOL appear to be a consequence of the structural modifications caused by the incorporation of cholesterol molecules into the DMPC monolayer (Fig. 5.5.2).

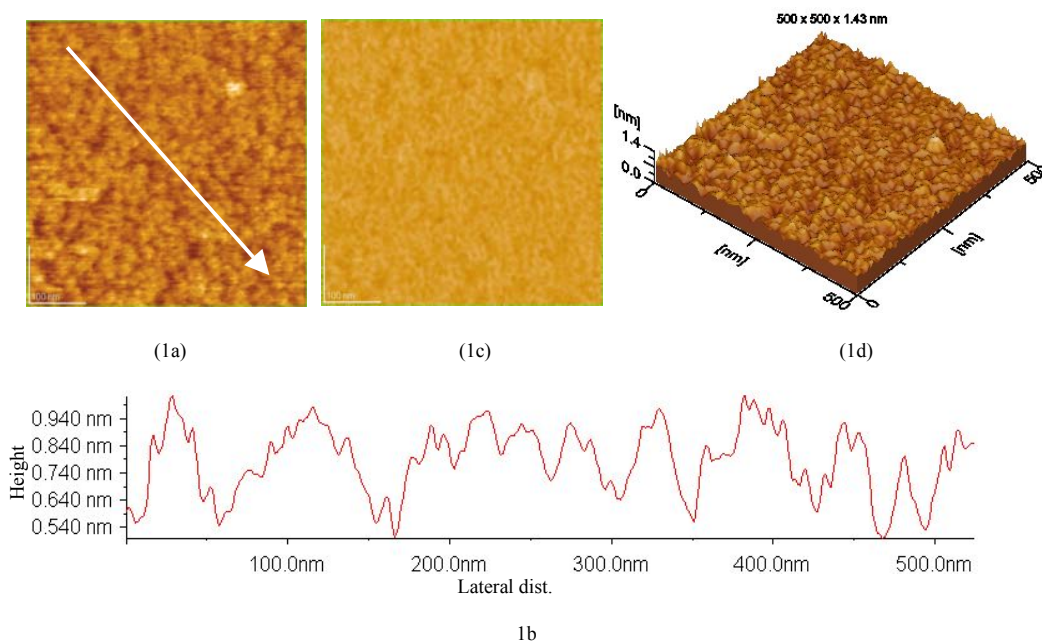


Fig.5.5.2. The AFM images for mixed DMPC:CHOL (4:1) monolayers, vertically transferred on mica at constant surface pressure of about 20 mN/m, for the scanned area: 500 x 500 nm². (1a) 2D -topographic images; (1b) cross section profile along the arrow in image (1a); (1c) phase image; (1d) 3D-view of 2D -topographic image(1a).

This study shows that the strong interactions between DMPC and CHOL lead to well defined two-dimensional nanostructures, with very low surface roughness, which can have practical applications for biosensors fabrication. Also, these types of nanostructures seem plausible to occur in natural membranes and thus, can influence the protein distribution and protein function *in vivo* [201].

5.6.3. Collagen membranes morphology in presence of anti-cancer drugs

Type I collagen is the major fibrillar protein in the extracellular matrix and in connective tissues [215]. It is a protein of molecular mass about 300 kg/mol, length about 300 nm, diameter around 1.5 nm, abundant in bone, cartilages, ligaments, tendons and skin [217].

Structurally, it consists of three chains, twisted to form a semi-rigid helical structure, the so called collagen monomer. Non-helical parts (telopeptides) are found at the extremities of each monomer. It contains regions which are specifically recognized by cell-surface receptors, being therefore involved in biorecognition processes.

Chemically, each chain is constructed from repeated amino acid sequences glycine-X-Y, where X and Y positions may be occupied by any amino acid; frequently proline is in X position and hydroxyproline in Y position.

By the assembly of collagen monomers, characteristic band patterns with a periodicity of 67 nm (D banding pattern) along the fibril length are formed. Further linear (end to end) and lateral association (entwining of the structures) gives rise to microfibrils which can further assembly into large fibrillar structures and finally into fibers [203].

The collagen supramolecular assembly plays an important role in mechanical reinforcement of tissues, and in proliferation, migration, and signal transduction of adjacent cells.

The studies of collagen films mixed with anti-cancer drugs: FLU, DOX and LPA confirm the formation of supramolecular associations and their assembly in nanostructured films deposited on glass (Figs. 5.6.10 – 5.6.12). The supramolecular organization of collagen molecules shows that the anti-cancer drug is strongly bound to collagen fragments. We suggest that the binding between collagen and anti-cancer drug takes place through molecular recognition between the least ordered zone of collagen, named telopeptides, and anti-cancer drug leading to more ordered mixed networks. Evidently, the formation of hydrogen bonds between the anti-cancer drugs and the collagen matrix is also essential for the stability of the mixed networks observed in AFM images.

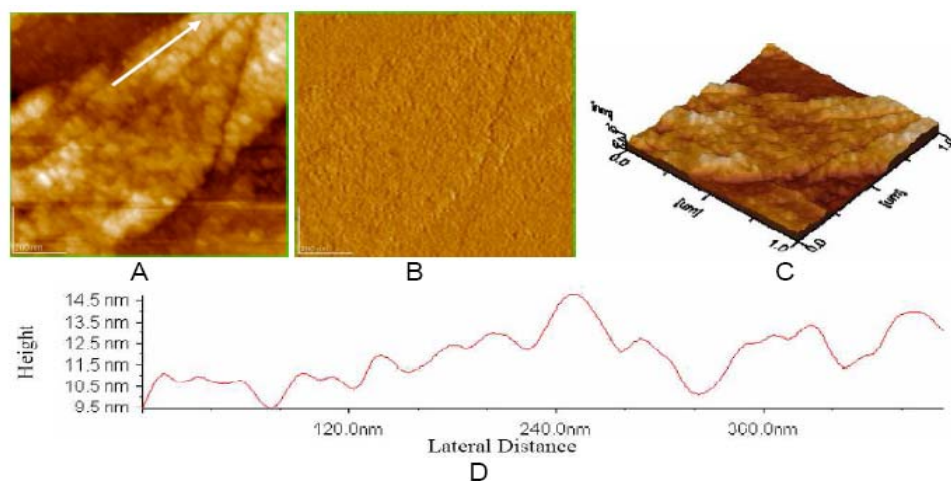


Fig 5.6.10. Collagen with 5-fluorouracil film on glass: A) 2D – topography; B) phase image; C) 3D – topography; D) profile of the cross section along the arrow in Fig. 5.6.10A. Scanned area $1 \times 1 \mu\text{m}^2$.

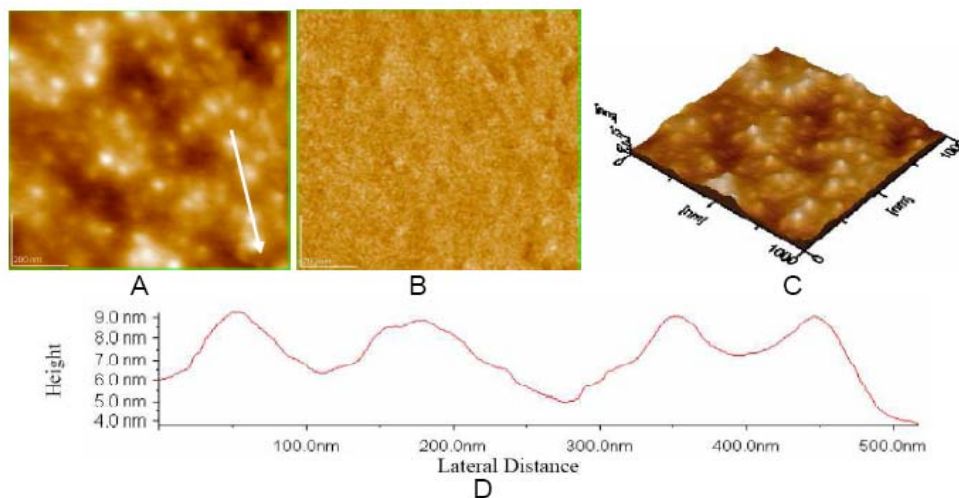


Fig.5.6.11. Collagen with doxorubicin film on glass: A) 2D – topography; B) phase image; C) 3D – topography; D) profile of the cross section along the arrow in Fig. 5.6.11A. Scanned area $1 \times 1 \mu\text{m}^2$.

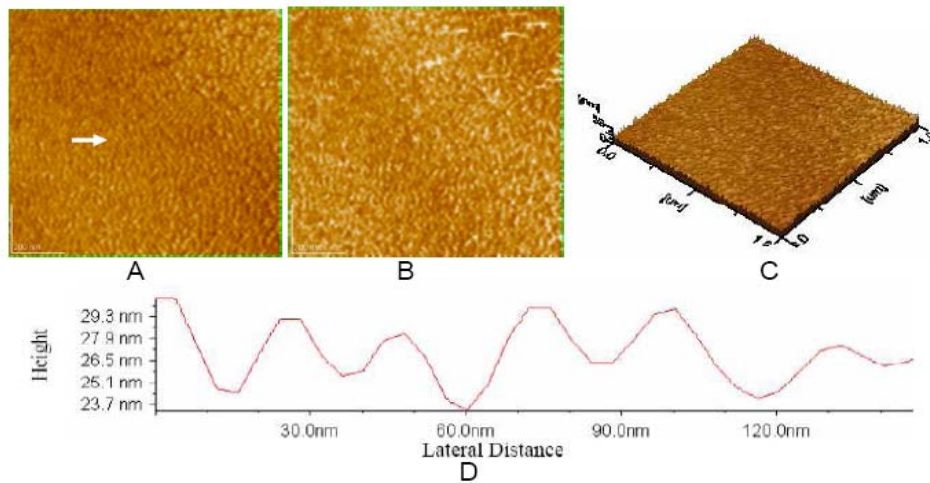


Fig.5.6.12. Collagen with lipoic acid film on glass: A) 2D – topography; B) phase image; C) 3D – topography; D) profile of the cross section along the arrow in Fig. 5.6.12A. Scanned area $1 \times 1 \mu\text{m}^2$.

The organization of proteins at surfaces is of increasing importance in a wide range of applications, including implant biocompatibility, cell adhesion and growth and biomaterials design. Such applications require a controlled morphology of the self-assembled dried layers of biomolecules at different surfaces, as in the case of biosensor devices, for which the distribution of proteins can influence the signal transduction [211] and cellular response [202, 211, 212].

6. Biological membranes. AFM observations of erythrocytes.

AFM images obtained for the whole cell surface morphology show that erythrocytes present a concave donut shape with an average lateral size about $8 \mu\text{m}$ in diameter and nearly $0.14 \mu\text{m}$ in depth of concave shape (Fig. 6.1.18). The nanostructure of normal human erythrocytes is featured by closely packed granules or particles with diameter of about 22 nm and almost uniformly distributed (Fig.6.1.19).

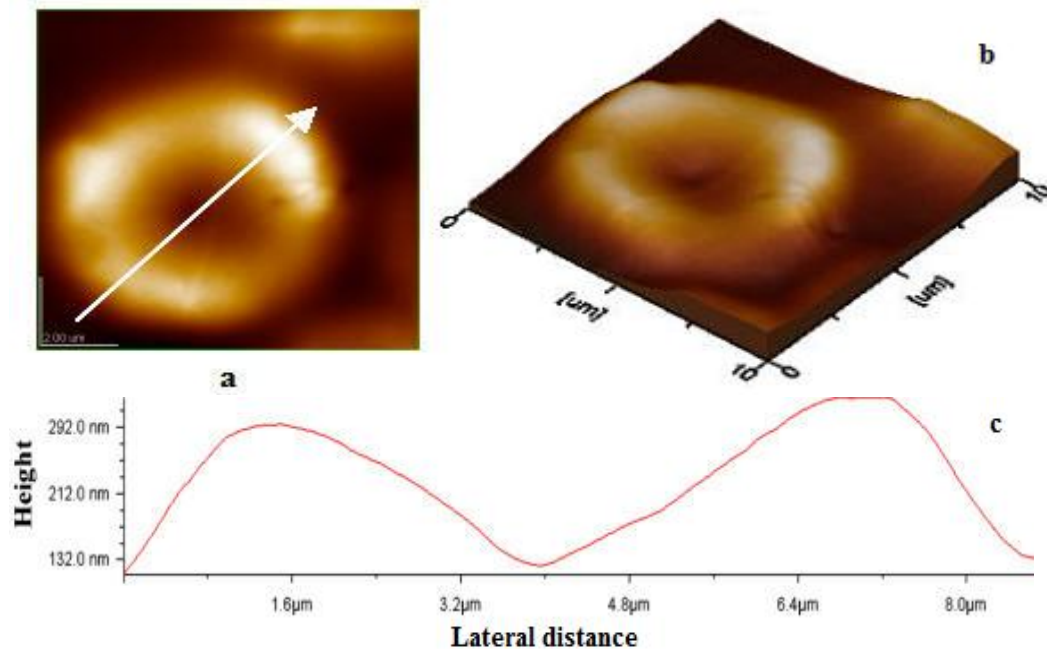


Fig. 6.1.18. AFM images of erythrocyte membrane surface, control sample: a) 2D – topography; b) 3D – topography; c) profile of the cross section along the arrow in image (a). Scanned area: $10 \mu\text{m} \times 10 \mu\text{m}$.

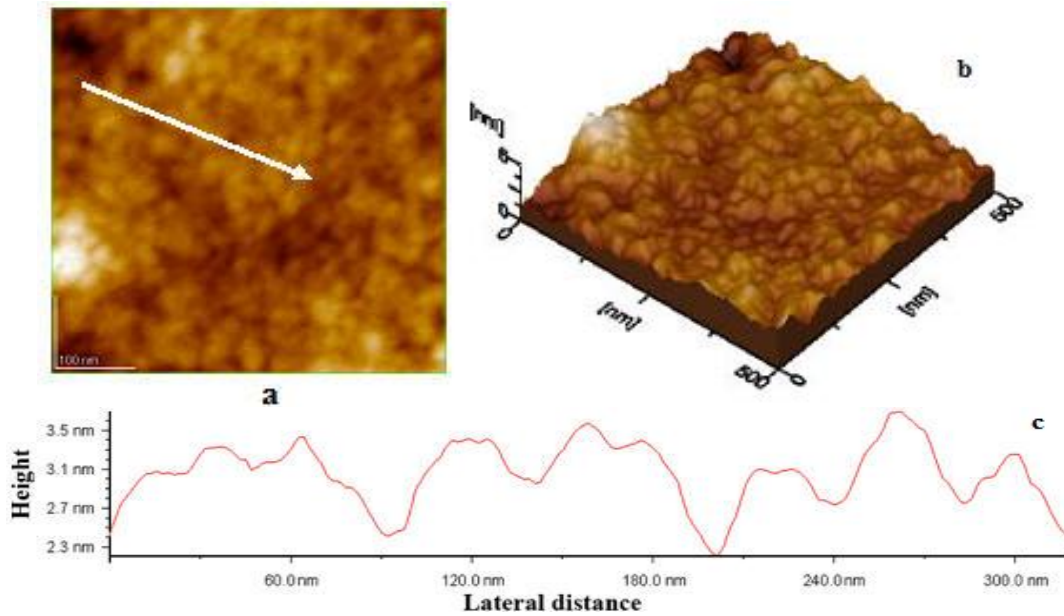


Fig. 6.1.19. AFM images of erythrocyte membrane surface, control sample: a) 2D – topography; b) 3D – topography; c) profile of the cross section along the arrow in image (a). Scanned area: 0.5 μm x 0.5 μm .

The granules probably correspond to membrane lipids well packed into the lipid part of the membrane surface in substantial agreement with lipid nanostructure found in monolayer membrane model [214, 259].

6.2. AFM observations of erythrocytes treated with procaine

The procaine effect on human erythrocytes was investigated by AFM at three procaine concentrations (see Table 6.2.1). The changes in surface morphology of erythrocytes membrane bring direct evidence on the procaine effect on the cell membrane at micro- and nanometer scale. The changes in the surface morphology of erythrocytes can be associated with the enlargement of surface granules, due to the aggregation of membranous particles within the cell surface, and domain structure formation appears to be induced by the increasing procaine concentrations (Fig. 6.2.7, 6.2.8).

Table 6.2.1. Erythrocytes size, concave depth, granules diameter, RMS on scanned areas and on cross profile through the erythrocytes membrane, for various P concentrations.

P conc., M	Scanned areas, μm^2	Cell size, μm	Concave depth, nm	Granu- les nm	RMS on scanned areas nm	RMS on cross profile, nm
5×10^{-7}	10 x 10	8	140	-	167	81.0
	1 x 1	-	-	24	1.0	0.4
	0.5 x 0.5	-	-	22	0.6	0.3
5×10^{-5}	10 x 10	8.3	240	-	175	108
	1 x 1	-	-	40	3.0	0.6
	0.5 x 0.5	-	-	40	2.53	0.6
5×10^{-4}	10 x 10	8.5	766	-	256	267
	0.5 x 0.5	-	-	80	9.0	2

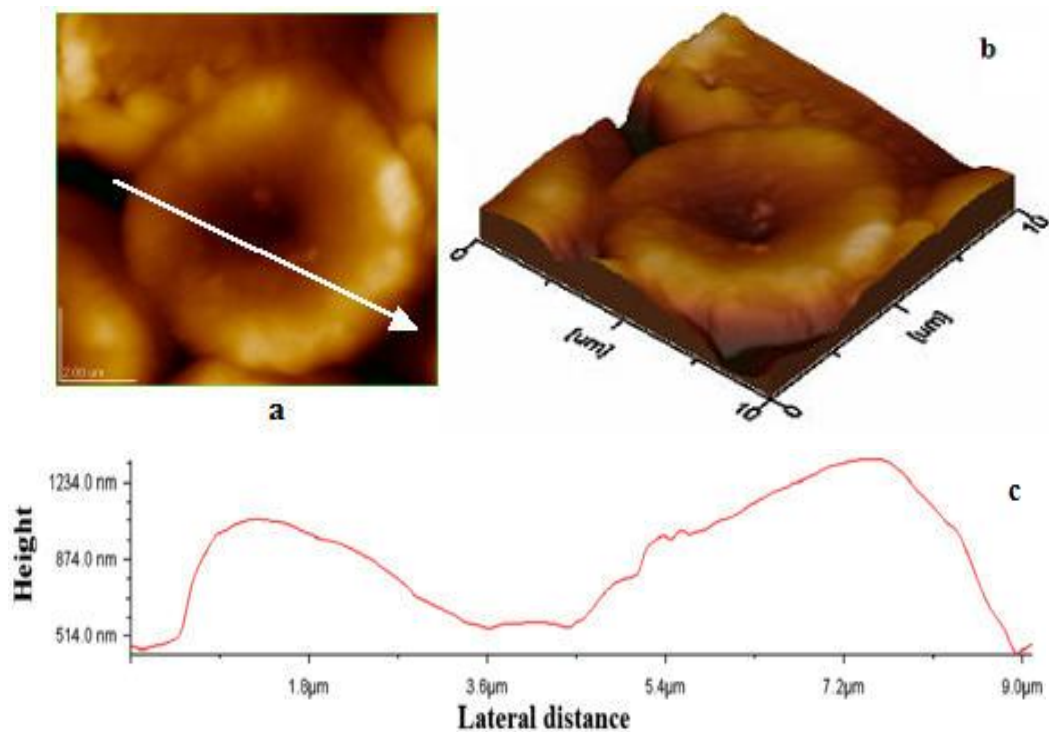


Fig. 6.2.7. AFM images of erythrocytes membrane in the presence of P $5 \times 10^{-4} M$. a) 2D-topography; b) 3D- topography; c) profile of the cross section along the arrow in image (a). Scanned area: $10 \times 10 \mu m^2$.

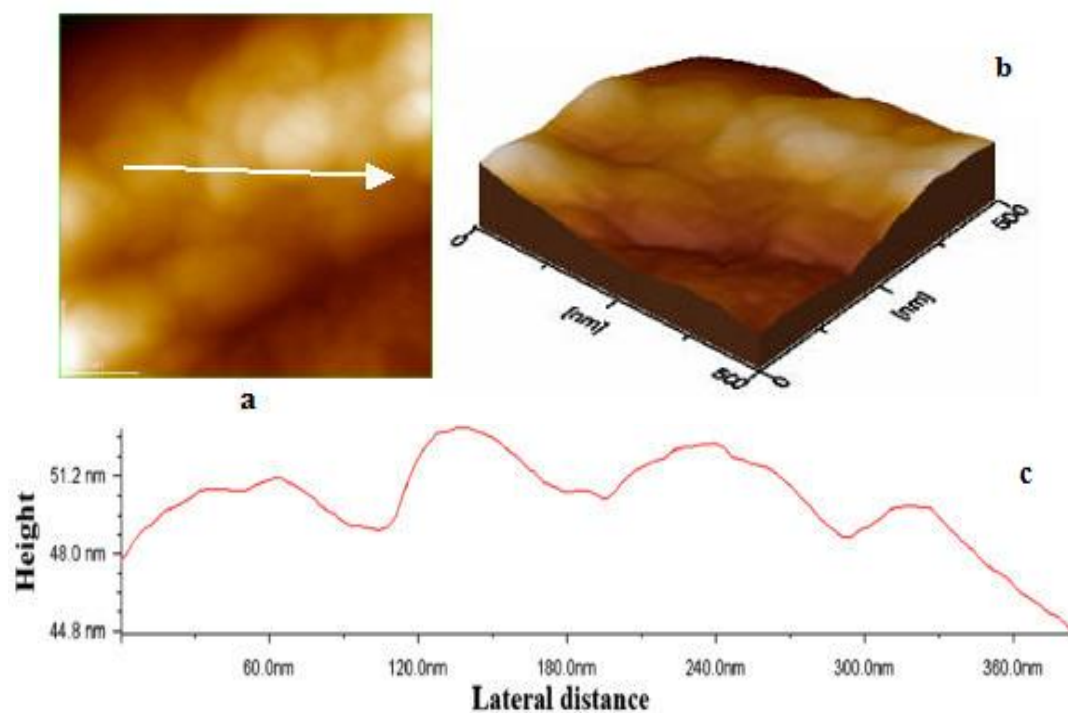


Fig. 6.2.8. AFM images of erythrocytes membrane surface in the presence of P $5 \times 10^{-4} M$. a) 2D-topography; b) 3D- topography; c) profile of the cross section along the arrow in image (a). Scanned area: $0.5 \times 0.5 \mu m^2$.

The procaine effect on erythrocytes membrane can be related to the increase stability of membrane surface due to specific interactions among procaine molecules and membrane components. The procaine effect on cell membrane might play an important role in anesthesia and in its function as a stimulant of a nervous system.

6.3. AFM observations of erythrocytes treated with deferoxamine

The examination of AFM images on human erythrocytes in the presence of DFO at different concentrations throw some light on the effect of drug on cell membranes (Table 6.3.1). The domain and pore structures mediated by DFO increased concentrations might be responsible for both enhanced surface aggregation and the perforation of erythrocytes membrane, leading to the interaction of DFO with proteins of the membrane cytoskeleton (Fig. 6.3.11, 6.3.14).

The mechanism of domain and pore formation or the perforation process induced by DFO at the highest concentration used can be discussed on the basis of specific interactions among drug and the membrane lipids.

The possibility of direct interaction of membrane proteins and DFO can contribute to the erythrocytes membrane major changes in the presence of drug at high concentration.

The molecular mechanism of the drug interaction with cells and the involvement of interfacial phenomena at the cell membrane are still not well understood, in spite of numerous investigations. As a first step the drugs action presume that the drug molecules modify the lipid membrane structure and thus, they may change the biological membrane properties.

The effect of drug concentrations on the structural and topographical characteristics of erythrocytes membranes were analyzed using AFM [259]. Since DFO is forms a very stable complex with iron (III), it is used for clinically removal of excess iron from blood and tissue and consequently, for the treatment of acute iron poisoning and iron overloaded anemia [264], as well as aluminium poisoning associated with chronic renal dialysis [265].

Table 6.3.1. Erythrocytes size, concave depth, granules diameter, RMS on scanned areas and on cross profile through the erythrocytes membrane, for various DFO concentrations.

DFO conc., M	Scanned areas, μm^2	Cell size, μm	Concave depth, nm	Granules nm	RMS on scanned areas, nm	RMS on cross profile, nm
5×10^{-7}	10 x 10	7.7	180	-	170	102
	0.5 x 0.5	-	-	30	2	0.6
5×10^{-6}	10 x 10	8.4	130	-	194	128
	5 x 5	-	-	-	111	106
	2.5 x 2.5	-	-	40-50	37.7	1.56
	1 x 1	-	-	40-50	5.16	1.25
5×10^{-5}	0.5 x 0.5	-	-	55-60	1.41	1.19
	10 x 10	8	300	-	265	161
	0.5 x 0.5	-	-	50	1	1
5×10^{-3}	15 x 15	-	-	680	32	32
	10 x 10	-	-	600	33	20
	5 x 5	-	-	400	25	10
	5 x 5	-	-	400	18	16
	2.5 x 2.5	-	-	230	14	8

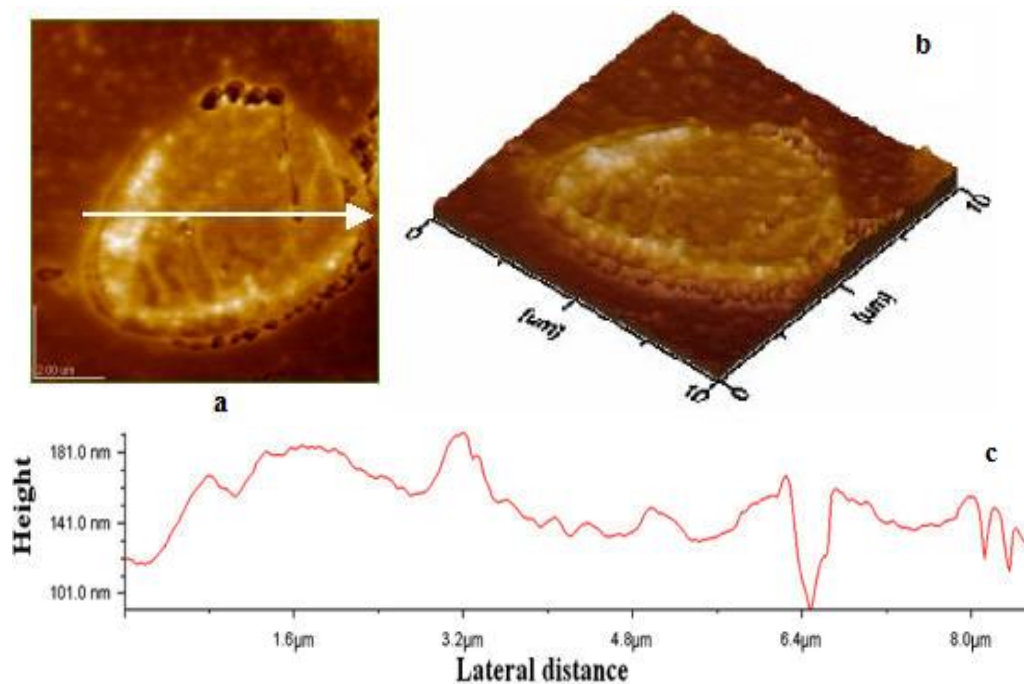


Fig.6.3.11. AFM images of erythrocytes membrane in the presence of DFO $5 \times 10^{-3} \text{M}$. a) 2D-topography; b) 3D- topography; c) profile of the cross section along the arrow in image (a). Scanned area: $10 \times 10 \mu\text{m}^2$.

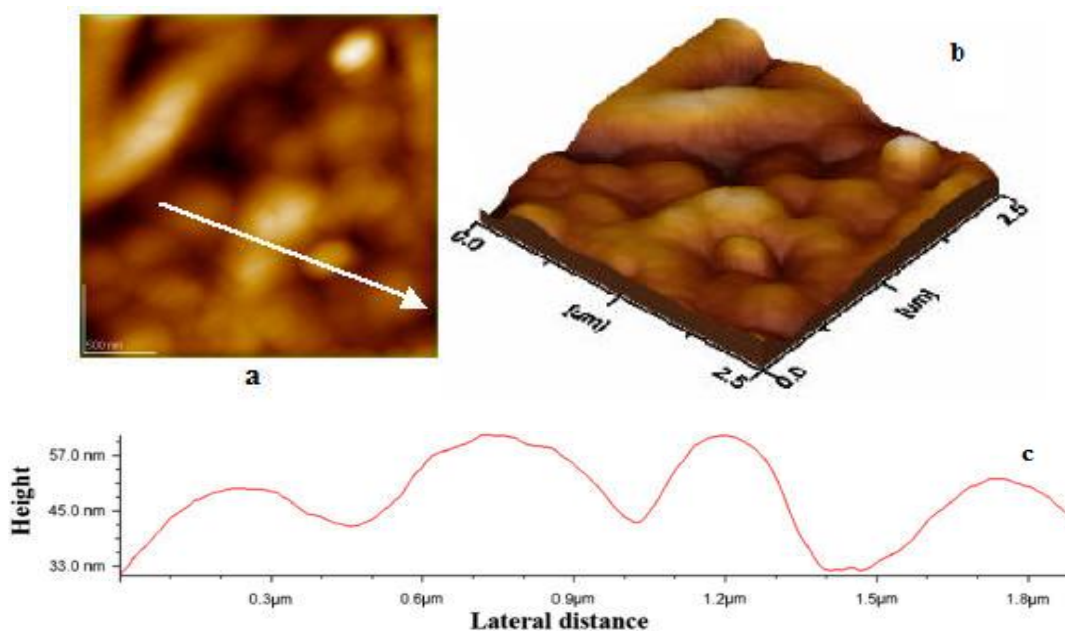


Fig.6.3.14. AFM images of erythrocytes membrane surface in the presence of DFO $5 \times 10^{-3} \text{M}$. a) 2D-topography; b) 3D- topography; c) profile of the cross section along the arrow in image (a). Scanned area: $2.5 \times 2.5 \mu\text{m}^2$.

Consequently, drug concentrations are very important and using AFM, now we are able to see, the effects of the drugs on the erythrocytes membrane and potential implication in medical treatment.

7. Conclusions

The behavior of lipid membranes and biomembranes in interaction with some chemicals (anesthetics, anticancer drugs) was studied to understand the mechanism of drug stability with application in drugs metabolism.

Fatty acid monolayers adsorbed (Gibbs) or spread (Langmuir) at the fluid interfaces were used as the first model to reproduce and to modeling the interactions of drugs with the cell membrane.

- a) Adsorption dynamics of stearic acid from benzene solutions and of tetracaine and dibucaine from aqueous solutions at the benzene/water interface, led us to obtain the following results:
- b) A new improved diffusion-controlled kinetic equation based on Ward and Tordai diffusion equation associated with a two dimensional state equation van der Waals type, which describes very well the adsorption dynamics was proposed;
 - o Diffusion coefficients, subsurface concentrations and the interaction parameter α , among the biosurfactant molecules, calculated with the new kinetic equation are close to the values obtained experimentally for different similar chemical compounds.
- c) Langmuir films of stearic acid spread on the aqueous subphase of pH 2 and the effect of drugs presence in aqueous subphase investigations, led to:
 - o Characterization the compression isotherm of pure stearic acid monolayers emphasizing the characteristic phases and the collapse mechanism.
 - o Study of the effects of subphase composition on SA monolayers in the presence of P and DFO. Stability of fatty acid Langmuir films was found to increase in the presence of drugs, by increasing their collapse pressure and the compression isotherms of SA with drugs are moved at higher molecular areas. In conclusion, appear a drug expansion effect on SA monolayer.

Mathematical modeling of compression isotherms of films of fatty acids was done by three methods:

1. State equation.
2. Interpolation by using spline function of compression isotherms.
3. Modeling compression isotherms using extended cubic spline function.

Mathematical modeling of compression isotherms has led to a fast and flexible computer program that can be used for faithful reproduction of the compression isotherms for different biocompounds for which there is little experimental data, ultimately achieving these films surface characteristics.

Phospholipid films spread (DPPC, DMPC) pure or mixed with certain chemical compounds (drugs, cholesterol) were studied, stating the following:

- o The collapse pressure of mixed films in presence of drugs increases, the highest value of collapse pressure is for the monolayer of DPPC with P, for the P concentration of 0.001 M.
- o Collapse areas for all lipid films are the same and independent of the presence of drugs in the film. This means that drugs are expelled from the monolayer when it is close to its collapse.
- o DMPC monolayer becomes more condensed in the presence of CHOL reflected by comparing the surface characteristics obtained from the compression isotherms of pure DMPC and CHOL monolayers and mixed film.

The behavior and morphology of thin films transferred on solid support by the Langmuir-Blodgett technique (LBT) using atomic force microscopy (AFM) were analyzed, noting that:

- o Collapse mechanism proposed for stearic acid is confirmed by the topographic images, phase and three-dimensional AFM images.

- Mixed films of SA with drugs are more stable and homogeneous than films of pure AS.
- DPPC films with drugs have the same stability as AS films with drugs, which mean strong interactions between these biocompounds by hydrogen bonds, van der Waals forces and electrostatic interactions.
- DMPC mixed with CHOL films have homogeneous structures with a low roughness. The homogeneity of the films due to interactions of DMPC with CHOL, which is incorporated into the DMPC monolayer film and increases the stability of mixed film.
- LB films of fatty acids and lipids have a long-term stability, observed in AFM images recorded a few days after transfer and repeated after a few months to a year. The results obtained provide information on possible modes of drug interaction with cell membranes.

We performed AFM observations on supramolecular associated collagen and studied the morphology of collagen membranes in the presence of anti-cancer drugs (doxorubicin, 5 - fluorouracil and lipoic acid) noting the following:

- Supramolecular organization of collagen molecules in the presence of anti-cancer drugs is due to fragments of collagen.
- The interaction of anticancer drugs with collagen provides valuable information on the transport of drugs targeted to certain tissues and membranes of the human body and collagen ability to deliver these drugs, optimizing their effect.

AFM observations of erythrocyte membrane structure and its changes caused by treatment with procaine and deferoxamine were performed and reached the following conclusions:

- Different types of drugs present in blood change the surface structure of erythrocyte membrane affecting interactions between lipids and proteins that enter into its composition.
- The purpose of this study was to determine the optimal drug concentration which does not produce cell destruction and is not harmful to the human body.

Ph D Thesis topic is related to the bioengineering of thin films. Strategy combining Langmuir-Blodgett technique with AFM investigations made it possible to analyze and model the interactions of chemical compounds with lipid membranes and biomembranes.

In this Ph D Thesis, the interactions of seven chemical compounds with lipid membranes and bimembranes were studied. The interactions between them and the membranes were modeled by modifying the concentrations of chemical compounds or by changing conditions of deposition and lipid transfer films studied in combination with chemical compounds. Interaction modeling between the studied biocompounds and the biological membranes, the behavior of pure lipid membranes and biomembrane structure were illustrated by AFM topographic images, phase images, and cross sections of topographic images.

8. Selected References

- [3] E. Chifu, "Chimia Coloizilor și a Interfețelor", Presa Universitară Clujeană, Cluj-Napoca (2000).
- [13] M. Tomoaia-Cotișel, J. Zsako, A. Mocanu, M. Lupea, E. Chifu, *J. Colloid Interface Sci.*, **117**, 464-476 (1987).
- [14] M. Tomoaia-Cotișel, E. Chifu, S. Jitian, I. Bratu, S. Bran, P. T. Frangopol, A. Mocanu, *Studia Univ Babeș-Bolyai, Chem.*, **35** (2), 17-24 (1990).
- [15] M. Tomoaia-Cotișel, *Progr. Colloid Polym. Sci.*, **83**, 155-166 (1990).
- [16] G. Gabrielli, *Adv. Colloid Interface Sci.*, **34**, 31-72 (1991).
- [17] M. Tomoaia-Cotișel, D. A. Cadenhead, *Langmuir*, **7**, 964-974 (1991).
- [33] K. S. Birdi, D. T. Vu, *Langmuir*, **10**, 623- 625 (1994).
- [34] Z. Lu, B. Zhang, Z. Ai, J. Huang, H. Nakahara, *Thin Solid Films*, **284-285**, 127-129 (1996).
- [36] K. Ekelund, E. Sparr, J. Engblom, H. Wennerstrom, S. Engstrom, *Langmuir*, **15**, 6950-6955 (1999).
- [40] G.L.Gaines Jr., "Insoluble Monolayers at Liquid/Gas Interfaces", Interscience Publishers, New-York, (1966).
- [42] M. Tomoaia-Cotișel, J. Zsako, E. Chifu, *Ann. Chim. (Rome)*, **71**, 189-200 (1981).
- [43] J. Zsako, M. Tomoaia-Cotișel, E. Chifu, A. Mocanu, P. T. Frangopol, *Gazz. Chim. Ital.*, **124**, 5-9 (1994).
- [48] M. Tomoaia-Cotișel, Gh. Tomoaia, A. Mocanu, **Vasilica-Daniela Pop**, N. Apetroaei, G. Popa, "Atomic force microscopy studies of Langmuir-Blodgett films. 2. Phase behavior of stearic acid monolayers", *Rev. Roum. Chim.*, **50**(5), 381-395 (2005).
- [49] M. Tomoaia-Cotisel, Gh. Tomoaia, **Vasilica-Daniela Pop**, A. Mocanu, O. Cozar, N. Apetroaei, G. Popa, "Atomic force microscopy studies of Langmuir-Blodgett films. 3. Phase behavior of dipalmitoyl phosphatidyl choline monolayers", *Rev. Roum. Chim.*, **50**(6), 471-478 (2005).
- [59] M.I. Sălăjan, A. Mocanu, M. Tomoaia-Cotișel, "Advances in Thermodynamics, Hydrodynamics and Biophysics of Thin Layers", University Press, Cluj-Napoca, (2004).
- [60] M. Tomoaia-Cotișel, Gh. Tomoaia, A. Mocanu, **Vasilica-Daniela Pop**, N. Apetroaei Gh. Popa, "Atomic force microscopy studies of Langmuir-Blodgett films. The effect of some drugs on dipalmitoyl phosphatidylcholine", *Studia Univ. Babeș Bolyai Chem.*, **49**(3), 141-152 (2004).
- [90] H. Hauser, I. Pascher, R. H. Pearson, S. Sundell, *Biochim. Biophys. Acta*, **650**, 21-51 (1981).
- [92] E. Sparr, L. Erikson, J. A. Bouwstra, K. Ekelund, *Langmuir*, **17**, 164-172 (2001).
- [96] J. T. Davies, E. K. Rideal, *Interfacial Phenomena*, Second Edition, New York, Academic Press, 154-216 (1963).
- [97] A. F. H. Ward, L. Torday, *J. Chem.Phys.*, **14**, 453-461 (1946).
- [98] P. Joos, G. Bleys, G. Petre, *J. Chem.Phys.*, **79**(2), 387-395 (1982).
- [99] G. Bleys, P. Joos, *J. Chem.Phys.*, **89**(6), 1027-1032 (1985).
- [100] P. Joos, G. Serrien, *J. Colloid Interface Sci.*, **127**(1), 97-103(1989).
- [104] E. Chifu, M. Sălăjan, J. Demeter-Vodnar, M. Tomoaia-Cotișel, *Rev. Roum. Chim.*, **32**, 683-691 (1987).
- [105] M. Tomoaia-Cotișel, I. Albu, E. Chifu, *Stud. Univ. Babeș-Bolyai Chem.*, **24**(2), 68-73 (1979).
- [106] E. Chifu, M. Tomoaia, E. Nicoară, A. Olteanu, *Rev. Roum. Chim.*, **23**, 1163-1169 (1978).
- [107] M.Tomoaia-Cotișel, J. Zsako, Gh. Tomoaia, A. Mocanu, **Vasilica-Daniela Pop** and E. Chifu, "Adsorption dynamics of some biosurfactants at the benzene/water interface", *Rev. Roum. Chim.*, **49** (5), 443-464, (2004).
- [111] J. Guastalla, *Cahiers Phys.*, **10**, 30 (1942); *J. Chim. Phys.*, **43**, 184-185 (1946).

- [112] L. Ter Minassian-Saraga, *J. Chim. Phys.*, **52**, 80-99 (1955).
- [113] E. Chifu, J. Zsako, M. Tomoaia-Cotișel, *J. Colloid Interface Sci.*, **95**, 346-354 (1983).
- [114] M. Tomoaia-Cotișel, E. Chifu, A. Mocanu, J. Zsako, M. Sălăjan, P.T. Frangopol, *Rev. Roum. Biochim.*, **25**, 227-237 (1988).
- [115] M. Tomoaia-Cotișel, J. Zsako, E. Chifu, *Stud. Univ. Babeș Bolyai Chem.*, **33**(2), 54-60 (1988).
- [119] M. Tomoaia-Cotișel, Gh. Tomoaia, A. Mocanu, **Vasilica-Daniela Pop**, N. Apetroaei and Gh. Popa, “**Atomic force microscopy studies of Langmuir-Blodgett films. I. Structures of collapsed stearic acid monolayers**”, *Studia Univ. Babeș Bolyai Chem.*, **49**(2), 167-181, 2004.
- [120] P. Baglioni, G. Gabrielli, G. G. T. Guarini, *J. Colloid Interface Sci.*, **78**, 347-355 (1980).
- [121] M. Tomoaia-Cotișel, J. Zsako, E. Chifu, D. A. Cadenhead, H. E. Ries, Jr., „Progress in Photosynthesis Research”, Edited by J. Biggins, Martinus Nijhoff Publishers, Vol. **2**, Chapter 4, 333-337, (1987).
- [122] M. Tomoaia-Cotișel, J. Zsako, A. Mocanu, I. Albu, E. Chifu, *Studia Univ. Babeș Bolyai, Chem.*, **32** (1), 58-67 (1987).
- [123] M. Tomoaia-Cotișel, J. Zsako, E. Chifu, D. A. Cadenhead, *Langmuir*, **6**, 191-197 (1990).
- [124] D. Vollhardt, U. Retter, *J. Phys. Chem.*, **95**, 3723-3724(1991).
- [125] J. Zsako, M. Tomoaia-Cotișel, E. Chifu, *J. Colloid Interface Sci.*, **102**, 186-205 (1984).
- [133] J. Zsako, M. Tomoaia-Cotișel, E. Chifu, A. Mocanu, P. T. Frangopol, *Biochim. Biophys. Acta*, **1024**, 227-232 (1990).
- [135] E. Sparr, K. Ekelund, J. Engblom, S. Engstrom, H. Wennerstrom, *J. Am. Chem. Soc.*, **121**, 486-487 (1999).
- [136] S. Ye, H. Noda, S. Morita, K. Uosaki and M. Osawa, *Langmuir*, **19**, 2238-2242 (2003).
- [137] M. Tomoaia-Cotișel, Gh. Tomoaia, **Vasilica-Daniela Pop**, A. Mocanu, “**AFM studies on membrane phospholipids in presence of drugs**”, *The 3rd International Workshop – Scanning Probe Microscopy Life Sciences*, Berlin, October 13, 2004, Poster 25, publish on internet.
- [139] J. M. Boggs, *Biochim. Biophys. Acta*, **906**, 353-404 (1987).
- [146] A. Cavalli, G. Borissevitch, M. Tabak, O. N. Oliveira Jr., *Thin Solid Films*, **284-285**, 731-734 (1996).
- [147] Z. Kozarak, B. Cosovic, D. Mobius, M. Dobric, *J. Colloid Interface Sci.*, **226**, 210-217 (2000).
- [148] A. Mocanu, Gh. Tomoaia, C.-R. Ispas, O.-C. Boroștean, D. Dubert, **Vasilica-Daniela Pop**, L. D. Boboș, M. Tomoaia-Cotișel, “**Two-dimensional nanostructures of dimyristoyl phosphatidylcholine and cholesterol at different interfaces**”, *Micro and Nanoengineering*, **9**, Romanian Academy Press, 178-191 (2006).
- [150] Y. Tagami, H. Ikigai, Y. Oishi, *Colloids Surfaces A: Physicochem. Eng. Aspects*, **284/285**, 475-479 (2006).
- [151] M. Tomoaia-Cotișel, E. Chifu, *J. Colloid Interface Sci.*, **95**, 355-361 (1983).
- [152] M. Tomoaia-Cotișel, J. Zsakó, A. Mocanu, E. Chifu, P.J. Quinn, *Biochim. Biophys. Acta*, **942**, 295-304 (1988).
- [171] B. W. MacArthur, J. C. Berg, *J. Colloid Interface Sci.*, **68** (2), 201-213(1979).
- [180] K. Ichida, F. Yoshimoto, T. Kiyono, *Computing*, **16**, 329-338 (1976).
- [181] F. Yoshimoto, „Studies on Data Fitting with Spline Functions”, Ph. D. Thesis, Kyoto University, Japan, 1977.
- [182] G. Micula, „Funcții spline și aplicații”, Ed. Tehnică, București, 1978.

- [188] M. Tomoaia-Cotișel, J. Zsako, E. Chifu, A. Mocanu, P. T. Frangopol, P. J. Quinn, *J. Rom. Colloid Surface Chem. Assoc.*, **2** (3-4), 30-36 (1997).
- [189] M. Tomoaia-Cotișel, A. Mocanu, J. Zsako, T. Oproiu, A. Aldea, P. J. Quinn, *J. Rom. Colloid Surface Chem. Assoc.*, **3**(2) 5-11 (1999).
- [190] M. Tomoaia – Cotișel, J. Zsako, E. Chifu, P. J. Quinn, *Chem. Phys. Lipids*, **50**, 127-133 (1989).
- [191] M. Tomoaia-Cotișel, J. Zsako, E. Chifu, P. J. Quinn, *Chem. Phys. Lipids*, **34**, 55-64 (1983).
- [195] P. Ehrenfest, *Proc. Akad. Sci. Amsterdam*, **36**, 147-153 (1933).
- [198] M. Tomoaia-Cotișel, **Vasilica-Daniela Pop**, Gh. Tomoaia, A. Mocanu, Cs. Racz, C. R. Ispas, O. Pascu, O. C. Boroštean, , “**Atomic force microscopy studies of Langmuir-Blodgett films. 4. The influence of aluminium substrate on dipalmitoyl phosphatidylcholine nanolayers**”, *Studia Univ. Babeș-Bolyai, Chem.*, **50**(1), 23-37, (2005).
- [201] A. Mocanu, Gh. Tomoaia, C.-R. Ispas, O.-C. Boroštean, D. Dubert, **Vasilica-Daniela Pop**, L. Boboș and M. Tomoaia-Cotișel, “**Two-dimensional nanostructures of dimyristoyl phosphatidylcholine and cholesterol at different interfaces**”, in *Convergence of Micro-Nano-Biotechnologies*, Series in *Micro and Nanoengineering*, **Volume 9**, Romanian Academy Press, București, 178 –191, 2006.
- [202] Gh. Tomoaia, **Vasilica-Daniela Pop-Toader**, A. Mocanu, O. Horovitz, L. D. Bobos, M. Tomoaia-Cotișel, “**Supramolecular organization and nanostructuring of collagen and anticancer drugs**”, *Studia Univ. Babeș-Bolyai, Chem.*, **52**(4), 2007.
- [203] Gh. Tomoaia, M. Tomoaia-Cotișel, A. Mocanu, O. Horovitz, L. D. Boboș, M. Crișan, I. Petean, *J. Optoelectron. Adv. Mat.*, **10** (4), 961-964 (2008).
- [211] F. A. Denis, P. Hanarp, D. S. Sutherland, J. Gold, C. Mustin, P. G. Rouxhet, Y. F. Dufrene, *Langmuir*, **18**, 819-828 (2002).
- [212] K. Kato, G. Bar, H.-J. Cantow, *Eur. Phys. J.*, **E6**, 7-14 (2001).
- [214] M. Tomoaia-Cotișel, A. Mocanu, N. Leopold, M. Vasilescu, V. Chiș, O. Cozar, *J. Optoelectron. Adv. Mat.*, **9**, 637-640 (2007).
- [215] E. Gurdak, P. C. Rouxhet, C. C. Dupont-Gillain, *Colloid Surfaces B: Biointerfaces*, **52**, 76 (2006).
- [217] C.C. Dupont-Gillain, I. Jacquemart, P. G. Rouxhet, *Colloids Surfaces B: Biointerfaces*, **43** (3-4), 179-186 (2005).
- [221] M. Tomoaia-Cotișel, A. Mocanu, G. Tomoaia, J. Zsako and T. Yupsanis, *J. Roum. Assoc. Colloid Surface Chem.*, **4**, 5-12 (2001).
- [259] M. Tomoaia- Cotișel, **Vasilica-Daniela Pop-Toader**, U. V. Zdrenghia, Gh. Tomoaia, O. Horovitz, A. Mocanu, „ **Desferal effect on human erythrocyte membrane. An atomic force microscopy analysis.**”, *Studia Univ. Babeș Bolyai, Chem.*, **54** (4), 285-296 (2009).
- [264] W. Banner Jr., T. G. Tong, *Pediatrics Clinics of North America*, **33**, 393-409 (1986).
- [265] J. P. Day, P. Ackrill, *Therapeutic Drug Monitoring*, **15**, 602-607 (1993).

9. List of original publications

A. PAPERS

- 1) M.Tomoaia-Cotișel, A. Mocanu, **Vasilica-Daniela Pop**, D.T.Pleșa, S.Pleșa and I. Albu, "Equations of state for films of fatty acids at the air/water interface", *Proceedings of The VII-th Symposium of Colloid and Surface Chemistry*, București, 2002, pp.42-47.
- 2) M.Tomoaia-Cotișel, J. Zsako, Gh. Tomoaia, A. Mocanu, **Vasilica-Daniela Pop** and E. Chifu, "Adsorption dynamics of some biosurfactants at the benzene/water interface", *Rev. Roum. Chim.*, **49** (5), 443-464, mai 2004.
- 3) M.Tomoaia-Cotișel, Gh. Tomoaia, A. Mocanu, **Vasilica-Daniela Pop**, N. Apetroaei and Gh. Popa, "Atomic force microscopy studies of Langmuir-Blodgett films. I. Structures of collapsed stearic acid monolayers", *Studia Univ. Babeș-Bolyai, Chem.*, **49**(2), 167-181, 2004.
- 4) M.Tomoaia-Cotișel, Gh. Tomoaia, **Vasilica-Daniela Pop**, A. Mocanu, O. Cozar, N. Apetroaei and Gh. Popa, "Atomic force microscopy studies of Langmuir-Blodgett films. The effect of some drugs on dipalmitoyl phosphatidylcholine", *Studia Univ. Babeș-Bolyai, Phys.*, **49**(3), 141-152, 2004.
- 5) M.Tomoaia-Cotișel, Gh. Tomoaia, **Vasilica-Daniela Pop**, A. Mocanu, "**AFM studies on membrane phospholipids in presence of drugs**", The 3rd International Workshop – Scanning Probe Microscopy Life Sciences, Berlin, October 13, **Poster 25**, published on internet, **2004**.
- 6) M.Tomoaia-Cotișel, Gh. Tomoaia, **Vasilica-Daniela Pop**, A. Mocanu, N. Apetroaei and Gh. Popa, "Atomic force microscopy studies of Langmuir-Blodgett films. 2. Phase behavior of stearic acid monolayers", *Rev. Roum. Chim.*, **50** (5), 381-395, 2005.
- 7) M.Tomoaia-Cotișel, Gh. Tomoaia, **Vasilica-Daniela Pop**, A. Mocanu, O. Cozar, N. Apetroaei and Gh. Popa, "Atomic force microscopy studies of Langmuir-Blodgett films. 3. Phase behavior of dipalmitoyl phosphatidyl choline monolayers", *Rev. Roum. Chim.*, **50** (6), 473-480, 2005.
- 8) M.Tomoaia-Cotișel, **Vasilica-Daniela Pop**, Gh. Tomoaia, A. Mocanu, Cs. Racz, C. R. Ispas, O. Pascu and O. C. Boroștean, "Atomic force microscopy studies of Langmuir-Blodgett films. 4. The influence of aluminium substrate on dipalmitoyl phosphatidylcholine nanolayers", *Studia Univ. Babeș-Bolyai, Chem.*, **50**(1), 23-37, 2005.
- 9) **Vasilica-Daniela Pop**, "Metode moderne de investigare a interacțiunilor unor compusi chimici asupra membranelor lipidice și biomembranelor", *Rev. de Politică Științei și Scientometrie*, nr. special, ISSN 1582-1218, 1-10, 2005.
- 10) M.Tomoaia-Cotișel, Gh. Tomoaia, A. Mocanu, **Vasilica-Daniela Pop**, N. Apetroaei and Gh. Popa, "Structures of stearic acid monolayers studied as Langmuir-Blodgett films and atomic force microscopy", *Proceedings of the 8th Symposium on Colloid and Surface Chemistry*, Galați, June 3-5, 2005, 4 pages, published DVD file on CD.
- 11) A. Mocanu, Gh. Tomoaia, C.-R. Ispas, O.-C. Boroștean, D. Dubert, **Vasilica-Daniela Pop**, L. D. Boboș and M. Tomoaia-Cotișel, "Two-dimensional nanostructures of dimyristoyl phosphatidylcholine and cholesterol at different interfaces", in *Convergence of Micro-Nano-Biotechnologies*, Series in *Micro and Nanoengineering*, **Volume 9**, Editors: Maria Zaharescu, Emil Burzo, Lucia Dumitru, Irina Kleps and Dan Dascalu, Romanian Academy Press, Bucharest, pp. 178 –191, 2006.
- 12) Gh. Tomoaia, **Vasilica-Daniela Pop-Toader**, A. Mocanu, O. Horovitz, L.D. Bobos, M. Tomoaia-Cotișel, "Supramolecular organization and nanostructuration of collagen and anticancer drugs", *Studia Univ. Babeș-Bolyai, Chem.*, **52**(4), 2007.

- 13) M. Tomoaia-Cotișel, **Daniela-Vasilica Pop-Toader**, U. V. Zdrengea, Gh. Tomoaia, O. Horovitz, A. Mocanu, "Desferal effect on human erythrocyte membrane. An atomic force microscopy analysis", *Studia Univ. Babeș-Bolyai, Chem.*, **54** (4), 2009.

B. BOOKS

- 14) E. Chifu, M. Tomoaia-Cotișel, I. Albu, A. Mocanu, M. I. Sălăjan, Cs. Racz and **Vasilica- Daniela Pop**, "Metode experimentale în chimia și biofizica coloizilor și a interfețelor", Presa Universitară Clujeană, 2004, pp.175, ISBN: 973-610-242-4.

C. COMMUNICATIONS

1. M. Tomoaia-Cotișel, A. Mocanu, **Vasilica-Daniela Pop**, D.T. Pleșa, S. Pleșa and I. Albu, "Equations of state for films of fatty acids at the air/water interface", The VII-th Symposium of Colloid and Surface Chemistry, București, septembrie 2002.
2. M. Tomoaia-Cotișel, Gh. Tomoaia, **Vasilica-Daniela Pop**, A. Mocanu, O. Cozar, N. Apetroaei and Gh. Popa, "Atomic force microscopy studies of Langmuir-Blodgett films. The effect of some drugs on dipalmitoyl phosphatidyl choline", The 1st International Conference – Advances Spectroscopies on Biomedical and Nanostructured Systems, Cluj-Napoca, September 19-22, 2004.
3. M. Tomoaia-Cotișel, Gh. Tomoaia, **Vasilica-Daniela Pop**, A. Mocanu, "AFM studies on membrane phospholipids in presence of drugs", The 3rd International Workshop – Scanning Probe Microscopy Life Sciences, Berlin, October 13, 2004.
4. M. Tomoaia-Cotișel, Gh. Tomoaia, A. Mocanu, **Vasilica-Daniela Pop**, N. Apetroaei and Gh. Popa, "Structures of stearic acid monolayers studied as Langmuir-Blodgett films and atomic force microscopy", The 8th Symposium on Colloid and Surface Chemistry, Galați, June 3-5, 2005.
5. A. Mocanu, **Vasilica-Daniela Pop**, C.R. Ispas, O. C. Boroștean, D. Dubert, Gh. Tomoaia, L. D. Boboș, O. Pascu, M. Tomoaia-Cotișel, „Two-dimensional nanostructures of dimyristoyl phosphatidylcholine and cholesterol at different interfaces”, The 5th National Seminar of Nanoscience and Nanotechnology”, București, March 2, 2006.

D. RESEARCH GRANTS

COORDINATOR

1. **Vasilica-Daniela Pop**, "Modern investigation methods of some chemical compounds interaction with lipid membranes and biomembranes", research grant CNCSIS 15/549, 2003.
2. **Vasilica-Daniela Pop**, "Modern investigation methods of some chemical compounds interaction with lipid membranes and biomembranes", research grant supplement CNCSIS 8/549, 2004.